HHS Public Access

Author manuscript

J Alzheimers Dis. Author manuscript; available in PMC 2024 July 01.

Published in final edited form as:

J Alzheimers Dis. 2024 ; 97(4): 1703–1726. doi:10.3233/JAD-230881.

Agent Orange Herbicidal Toxin-Initiation of Alzheimer-Type Neurodegeneration

Suzanne M. de la Monte[a,b,*], **Ming Tong**[b]

[a]Departments of Pathology and Laboratory Medicine, Neurology, and Neurosurgery, Rhode Island Hospital, Lifespan Academic Institutions, and the Warren Alpert Medical School of Brown University, Providence, RI, USA

[b]Department of Medicine, Rhode Island Hospital, Lifespan Academic Institutions, and the Warren Alpert Medical School of Brown University, Providence, RI, USA

Abstract

Background: Agent Orange (AO) is a Vietnam War-era herbicide that contains a 1 : 1 ratio of 2,4-dichlorophenoxyacetic acid (2,4-D) and 2,4,5-trichlorophenoxyacetic acid (2,4,5-T). Emerging evidence suggests that AO exposures cause toxic and degenerative pathologies that may increase the risk for Alzheimer's disease (AD).

Objective: This study investigates the effects of the two main AO constituents on key molecular and biochemical indices of AD-type neurodegeneration.

Methods: Long Evans rat frontal lobe slice cultures treated with 250 μg/ml of 2,4-D, 2,4,5-T, or both (*D* + T) were evaluated for cytotoxicity, oxidative injury, mitochondrial function, and AD biomarker expression.

Results: Treatment with the AO constituents caused histopathological changes corresponding to neuronal, white matter, and endothelial cell degeneration, and molecular/biochemical abnormalities indicative of cytotoxic injury, lipid peroxidation, DNA damage, and increased immunoreactivity to activated Caspase 3, glial fibrillary acidic protein, ubiquitin, tau, paired-helical filament phosphorylated tau, AβPP, Aβ, and choline acetyltransferase. Nearly all indices of cellular injury and degeneration were more pronounced in the *D* + T compared with 2,4-D or 2,4,5-T treated cultures.

Conclusions: Exposures to AO herbicidal chemicals damage frontal lobe brain tissue with molecular and biochemical abnormalities that mimic pathologies associated with early-stage AD-type neurodegeneration. Additional research is needed to evaluate the long-term effects of AO exposures in relation to aging and progressive neurodegeneration in Vietnam War Veterans.

[*]Correspondence to: Dr. Suzanne M. de la Monte, MD, MPH, Department of Medicine, Rhode Island Hospital, Providence, RI, 02908, USA. Fax: +1 401 444 2939; Suzanne_DeLaMonte_MD@Brown.edu.

CONFLICT OF INTEREST

Suzanne de la Monte is an Editorial Board Member of this journal but was not involved in the peer-review process nor had access to any information regarding its peer-review.

The other author has no conflict of interest to report.

Keywords

Agent Orange; Alzheimer's disease; brain; herbicide; neurodegeneration; neurons; pesticide; Vietnam Veterans; white matter; 2; 4-D; 2; 4; 5-T

INTRODUCTION

Neurodegenerative diseases, including Alzheimer's disease (AD), are primarily sporadic in their occurrences rather than distinctly genetic, drawing interest in the potential roles of lifestyle, environmental, and exposure-related co-factors responsible for their initiation, propagation, or exacerbation. Metabolic disorders contributing to cognitive impairment and AD-type neurodegeneration include obesity, diabetes mellitus, and non-alcoholic fatty liver disease [1]. Heavy chronic and binge alcohol exposures cause cognitive impairment, neuropsychiatric disorders, and dementia [2]. Herbicides and other toxin exposures have been linked to Parkinson's disease [3-6]. Environmental toxin (herbicide and pesticide) exposures are correlated with increased rates of sporadic motor neuron disease, particularly amyotrophic lateral sclerosis (ALS) [7, 8]. Chronic exposure to cycad toxins is believed to have been the cause of ALS-Parkinsonism-Dementia Complex of Guam, which was virtually abolished following public health interventions [9, 10].

The growing list of herbicides, pesticides, and preservatives that damage the nervous system and lead to long-term disabilities and diseases is of deep concern because the lack of awareness and therefore failure to implement preventive measures shorten productive lifespans, compromise quality of life, drive up healthcare costs, and threaten socioeconomic well-being. Worse yet are the exposures that occur for short-term gains vis-à-vis inadequate understanding of their long-term consequences. Examples include the widespread use of nitrates and nitrites to preserve and process foods while staving off Salmonellosis [11]. Chemical reactions between nitrates or nitrites and amine groups present in meats and fish lead to nitrosamine formation [12]. Nitrosamines in high concentrations are carcinogenic [13], but the long-term effects of low-concentration exposures include degenerative diseases that are rooted in insulin resistance, including cognitive impairment with AD-type neurodegeneration, diabetes, fatty liver disease, and obesity [11, 14, 15]. More recently, interest in the long-term adverse effects of Agent Orange exposures during the Vietnam War has grown as the affected U.S. Veteran population has aged with apparently higher rates of certain malignancies and chronic diseases [16-20].

Agent Orange is a synthetic defoliating herbicide that was widely used between 1965 and 1970 during the Vietnam War [20]. U.S. military personnel exposures occurred with aircraft spraying of enemy territory and the stationing of ground troops close to treated zones [20]. First, the teratogenic effects of Agent Orange were acknowledged years after the exposures, based on increased rates of severe birth defects and developmental disabilities in the offspring of healthy Vietnamese women who resided in Agent Orange sprayed areas [21, 22]. Next came the higher rates of newly diagnosed malignancies, cardiovascular disease, and diabetes mellitus in Agent Orange-exposed military personnel [23-26]. Furthermore, critical reviews and literature analyses revealed links between Agent Orange exposures

and later development of peripheral nervous system or central nervous system (CNS) degenerative diseases [27], and significantly higher rates and earlier onsets of dementia [28]. Although causal roles have been difficult to prove due to overlap with anticipated aging-associated pathologies, their higher rates, years after the exposures suggest that Agent Orange may have had indirect or “second hit” type long-term effects that promote or exacerbate aging-associated diseases. However, mechanistic studies are needed to solidify the links, better understand the process, and implement monitoring and interventional approaches.

Agent Orange exerts its toxic and degenerative effects on human nervous system cells [19, 27, 29-31]. Agent Orange contains equal proportions of 2,4-dichlorophenoxyacetic acid (2,4-D) and 2,4,5-trichlorophenoxyacetic acid (2,4,5-T), together with trace contaminants of 2,3,7,8-tetrachloro-p-dioxin (TCDD) [20]. Acute exposures to 2,4-D or 2,4,5-T occur by ingestion of contaminated foods, or breathing contaminated air. Efficient absorption through the gastrointestinal tract or lungs is followed by widespread distribution of 2,4-D and 2,4,5-T throughout the body prior to their excretion unchanged in urine [20, 32]. However, after repeated dosing, although the majority of chlorophenoxyacetic acids are excreted unchanged in urine, a significant proportion binds reversibly to plasma proteins and forms acid-hydrolyzable conjugates. Metabolites of 2,4,5-T such as N-(2,4,5- trichlorophenoxy-acetyl)-glycine have been identified. Furthermore, despite relatively rapid clearance after short-term exposures, repeated and high-dose exposures to 2,4,5-T or 2,4-D exert significant and broadly toxic effects on the liver, kidneys, fetus and offspring growth, development, viability, and neurobehavioral functioning [32, 33].

Regarding the nervous system, 2,4-D was shown to exert lipotoxic effects on myelin, gangliosides, and Schwann cells [34-38], threatening speed and efficiency of neuronal conductivity and possibly contributing to chronic peripheral neuropathy. Increased rates of Parkinson’s disease have been observed in farmers exposed to 2,4-D or 2,4,5-T [32], and Vietnam war veterans exposed to Agent Orange [20, 27, 30]. Furthermore, recent studies in immature CNS-derived human neuronal cells showed that short-term exposures to 2,4-D or 2,4,5-T differentially produce neurotoxic and early degenerative effects with altered expression of proteins that are dysregulated in AD [39]. The present work extends the observations made initially in transformed immature human CNS neuronal cells by examining the neurotoxic and degenerative responses to 2,4-D, 2,4,5-T, and combined 2,4-D+2,4,5-T (*D* + T) exposures on mitochondrial function, viability, stress, and markers of neurometabolic dysfunction and AD-type neurodegeneration using frontal lobe slice cultures from adolescent Long Evans rats. The rationale was that significant impairments related to these indices would provide evidence that Agent Orange exposures can initiate a deleterious path toward progressive neurodegeneration, including AD, motor neuron disease, peripheral polyneuropathies, and Parkinson’s disease [19] and that the adverse effects of combined exposures that mimic Agent Orange, would be additive or synergistic in driving neurodegeneration. It is also noteworthy that the molecular and cellular pathophysiological mediators of various types of neurodegeneration, including Parkinson’s disease, motor neuron disease, frontotemporal lobar degeneration, and Huntington’s disease share common pathways linked to mitochondrial dysfunction, oxidative stress, impaired neuronal viability, and dysregulated metabolism [40-43]. Therefore, the findings herein will likely have

relevance to the concept that adverse environmental exposures, including Agent Orange, can be linked to the pathogenesis of seemingly sporadic and varied forms of neurodegeneration [19].

MATERIALS AND METHODS

Reagents and resources

The purchased commercial antibodies used and RRID numbers are provided in Table 1. Thermo Fisher Scientific (Bedford, MA, USA) was the source of Superblock (TBS), bicinchoninic acid (BCA) reagents, Enzyme-Linked Immunosorbent Assay (ELISA) MaxiSorp 96-well plates, and Horseradish peroxidase (HRP)-conjugated secondary antibody. Life Technologies (Carlsbad, CA, USA) was the source of Amplex Red fluorophore and 4-Methylumbelliferyl phosphate (4-MUP). Vector Laboratories Inc. (Newark, CA, USA) was the source of alkaline phosphatase streptavidin, the Biotin Protein Labeling Kit, and the ImmPRESS Universal PLUS Polymer kit for immunohistochemical staining. Molecular Devices Corp. (Sunnyvale, CA, USA) was the source of the SpectraMax M5 microplate reader.

Experimental model

The Lifespan Institutional Animal Care and Use Committee (IACUC), Board Reference #500221 approved using rats for this research. Adolescent Long Evans rats were sacrificed at four weeks of age by isoflurane inhalation to generate fresh frontal lobe slice cultures (FLSCs) as described [44-46]. After chilling in ice-cold Hank's Balanced Salt Solution (HBSS), the frontal lobes were sliced at 250 μm intervals using a McIlwain tissue chopper (Mickle Laboratory Engineering Co. Ltd, UK). Slices separated under a dissecting microscope were cultured in 12-well Nunc plates (4 or 5 slices per well) containing Dulbecco's Modified Eagles Medium (DMEM) supplemented with 10% heat-inactivated fetal bovine serum (FBS), 1X MEM non-essential amino acids solution, 4 mM L-glutamine, 4.5 g/L glucose, 25 mM potassium chloride, 120 U/ml Penicillin, 120 μg/ml Streptomycin at 37°C in a 5% CO_2 incubator. After overnight incubation, the cultures were treated with vehicle (Veh), 250 μg/ml of 2,4-D, 2,4,5-T, or both for 24 h. Since 2,4-D and 2,4,5-T were solubilized in dimethyl sulfoxide (DMSO) and further diluted with serum-free DMEM, vehicle control cultures were treated with the same content of DMSO diluted in DMEM. The 2,4-D and 2,4,5-T treatments were guided by our recent publication [39] and previous *in vitro* studies in a range of cell types [38, 47-49]. However, the concentrations used for *in vitro* experiments may have differed from those used in the herbicide sprays [50]. Direct comparisons with historical human exposures to Agent Orange are not possible, particularly since most of the earlier research was focused on TCDD. On the other hand, the doses used herein were substantially lower than the 100 or 200 mg/kg daily administrations employed for *in vivo* rodent models [35, 36].

At the end of the experiment, culture supernatants were harvested to measure glucose 6 phosphate dehydrogenase (G6PD) release as a measure of cytotoxicity using the Vibrant Cytotoxicity Assay Kit (V-23111) according to the manufacturer's protocol (Molecular Probes-Thermo Fisher Scientific, Eugene OR). Results were normalized to Hoechst

H33342 fluorescence to adjust for cell loss resulting from cytotoxicity. To analyze protein expression, the tissue slices were homogenized in a weak lysis buffer containing protease and phosphatase inhibitors [51], and supernatants resulting from a 15-minute,14000rpm centrifugation at 4°C were snap frozen for later analysis. The bicinchoninic acid (BCA) assay measured sample protein concentrations.

For histopathological and immunohistochemical staining studies, two slices from each culture well were fixed in 10% neutral buffered formalin, embedded en face in paraffin and sectioned at a thickness of 5 μm. Prior to staining, the slides were heated at 60°C for 20 min to melt the wax. The tissue sections were then deparaffinized and hydrated through two changes each of xylenes followed by graded ethanol solutions (100%, 95%, 70%), and then distilled water. Hematoxylin and eosin (H&E) staining was performed using the Abcam ab245880 protocol [https://www.abcam.com/ps/products/245/ab245880/documents/H&E-Staining-Kit-protocol-book-v2-ab245880%20.pdf]. Adjacent sections were immunostained with antibodies to myelin-associated glycoprotein 1 (MAG1), glial fibrillary acidic protein (GFAP), and phospho-tau (paired-helical filament) as previously described [52, 53]. For immunohistochemical staining, de-waxed, rehydrated sections were treated with 0.3% H_2O_2 in methanol for 30 min to quench endogenous peroxidase activity. Non-specific binding sites were masked with blocking solution provided with the ImmPRESS HRP Universal PLUS Polymer kit, Peroxidase (Vector Laboratories, Inc. Newark, CA, USA). The tissues were then incubated with primary antibodies overnight incubation with primary antibody at 4°C. Immunoreactivity was detected with peroxidase-conjugated polymer and 3-3'-diaminobenzidine (Vector Laboratories) according to the manufacturer's protocol. The sections were counterstained with Hematoxylin, dehydrated through graded ethanol solutions, cleared in xylenes, and preserved under coverglass. Under code, the slides were evaluated by light microscopy and then photographed using standardized conditions to qualitatively illustrate the distributions of immunoreactivity quantified by ELISA.

Biomarker indices

The studies focused on the effects of 2,4-D, 2,4,5-T, and their combined exposures (*D* + T) in relation to AD pathology-associated protein expression, oxidative stress or injury, and mitochondrial function. Immunoreactivity was measured for tau, phospho-tau (paired helical filament, PHF), choline acetyltransferase (ChAT), acetylcholinesterase (AChE), amyloid-beta protein precursor (AβPP), Aβ fragment of AβPP, GFAP, ubiquitin (UBQ), 8-hydroxydeoxyguanosine (8-OHdG), 4-hydroxy-2-nonenal (HNE), and activated Caspase 3. Glyceraldehyde-3-phosphate dehydrogenase (GAPDH), an insulin-responsive enzyme [54], served as a marker of metabolic integrity. Proliferating cell nuclear antigen (PCNA) marked cellular proliferation responses. The five mitochondrial protein complexes (Complex I-V) were measured as indices of oxidative mitochondrial function. Large acidic ribosomal protein (RPLPO) served as an internal loading control [55-58] for normalizing the levels of specific immunoreactivities in each sample [44, 51, 59]. The antibody descriptions, sources, concentrations, and validation references are provided in Table 2.

Duplex ELISAs

This assay quantified immunoreactivity in FLSC homogenates, including 6 independent cultures per group with duplicate measurements. In brief, the protein samples (50 ng each) were adsorbed overnight at 4°C to the bottom surfaces of 96-well MaxiSorp plates. Superblock (TBS) Buffer masked nonspecific sites. Primary antibody incubations (see Table 1) were carried out overnight at 4°C, and after buffer rinsing, immunoreactivity was detected with HRP-conjugated secondary antibody and the Amplex UltraRed soluble fluorophore. Fluorescence intensity was measured in a SpectraMax M5 (Ex 530 nm/Em 590 nm). RPLPO immunoreactivity, measured in the same plates with biotinylated anti-RPLPO and streptavidin-conjugated alkaline phosphatase and 4-MUP (*Ex*360 nm/*Em*450 nm), was used to calculate relative levels of target protein expression in each well. The mean relative protein expression levels, i.e., ratios of specific protein/RPLPO, were used for inter-group statistical comparisons.

Statistics

Inter-group comparisons were made using one-way analysis of variance (ANOVA) with Tukey post hoc multiple comparisons tests (GraphPad Prism 10.0, San Diego, CA). The F-ratios, degrees of freedom, and p-values with significant ($p < 0.05$) differences highlighted are shown in Tables 2-4. The significant post hoc test results are depicted in the graphs (Figs. 4-7).

RESULTS

Histopathological features of 2,4-D and 2,4,5-T exposures

Formalin-fixed, paraffin-embedded, H&E-stained rat FLSC sections were examined from each culture well to assess the qualitative histopathological changes resulting from 2,4-D, 2,4,5-T, or both treatments. Representative images are shown in Fig. 1. H&E stained sections of control cases revealed relatively intact neuronal, parenchymal, and vascular architectures in cortical regions (Figs. 1A, 2A, 2B), and abundant white matter oligodendrocyte nuclei (Figs. 1B, 2C), intact vascular endothelial cells (Figs. 1B, 2C, 2D), uniform parenchyma except for mild edema, and scattered astrocytes (Figs. 1B, 2C, 2D). The 2,4-D treatment (Figs. 1C, 1D, 2E-2H) had striking injurious/degenerative effects on cortical neurons resulting in cytoplasmic eosinophilia with nuclear hyperchromasia or apoptosis (Figs. 1C, 2E), vascular wall necrosis in both cortex and white matter (Figs. 1D, 2F, 2H), architectural disruption in white matter (Figs. 1D, 2G, 2H), and reduced abundance of oligodendrocytes (Figs. 1D, 2G, 2H). The treatment with 2,4,5-T (Figs. 1E, 1F, 2I-2L) caused similar degrees of cortical neuronal injury/degeneration as observed with 2,4-D but with foci of conspicuous neuronal loss, focal vascular wall necrosis, and parenchymal degeneration (Figs. 1E, 2I, 2J) and white matter pathology associated with prominent activation of astrocytes, patchy vasculopathy, and modest oligodendrocyte injury or loss (Figs. 1F, 2K, 2L). The modest injury of oligodendrocytes was characterized by cytoplasmic eosinophilia or nuclear apoptosis. Treatment with 2,4,5-T severely disrupted the white matter matrix architecture (Fig. 2L). The D + T herbicidal toxin treatments (Figs. 1G, 1H, 2M, 2P) appeared to have additive effects on cortical neuronal injury and degeneration with conspicuous apoptosis (Figs. 1G, 2M), cortical and white matter vascular wall necrosis

(Figs. 1H, 2N, 2P), activated hypertrophic astrocytes (Fig. 2O, 2P), and degeneration of white matter parenchyma associated with abundant punctate/granular processes reminiscent of diffusely swollen axons (Figs. 1H, 2O, 2P).

Immunohistochemical staining was used for qualitative assessments of glial pathology to complement the quantitative results obtained by ELISA. Representative results are shown in Fig. 3. Immunohistochemical staining for myelin-associated glycoprotein (MOG) (Fig. 3A-3D) and GFAP (Fig. 3E-3H) were used to further assess the integrity of white matter and activation of astrocytes in response to the 2,4-D, 2,4,5-T, and *D* + T treatments. In control cultures, abundant MOG immunoreactivity was detected throughout white matter (Fig. 3A), whereas following 2,4-D, 2,4,5-T, or *D* + T treatment, the levels of MOG immunoreactivity were markedly reduced. In addition, treatment with 2,4-D or *D* + T resulted in striking coarse punctate MOG immunoreactivity which may have corresponded to diffuse axonal injury with swelling. GFAP immunoreactivity was largely associated with white matter vessels in control samples (Fig. 3E). Treatment with 2,4-D or 2,4,5-T resulted in increased densities of GFAP-reactive astrocytes with fibrillary cytoplasm (Fig. 3F, 3G). Treatment with *D* + T resulted in prominently increased GFAP+ fibrillary astrocytes and fibrils with intense levels of immunoreactivity (Fig. 3H).

Cytotoxic effects of 2,4-D and 2,4,5-T (Fig. 4)

Dead or dying cells release cytoplasmic G6PD and other enzymes like lactate dehydrogenase (LDH) into the surrounding culture medium. Agent Orange herbicidal toxin exposures had significant effects on FLSC cytotoxicity as demonstrated with the Vibrant Cytotoxicity Assay (G6PD release assay) (Table 3). The mean levels of G6PD corrected for DNA content (H33342 fluorescence) were significantly elevated in culture supernatants from the 2,4-D- and 2,4,5-T-treated relative to vehicle control cultures (Fig. 3). In contrast, the combined *D* + T treatment was not significantly elevated. Linear trend analysis for shifts in G6PD/H33342 from Vehicle to 2,4-D, to 2,4,5-T, to *D* + T treatments was not significant, but the non-linear trend ($r^2 = 0.6551$) was significant ($p = 0.011$), corresponding with the inverted U-shaped trendline (See Fig. 4).

Effects of 2,4-D and 2,4,5-T on indices of oxidative damage (Table 3 and Fig. 5)

Immunoreactivity to HNE, 8-OHdG, ubiquitin, and activated Caspase 3 served as markers of lipid peroxidation, nucleic acid damage, unfolded or misfolded protein responses and pro-apoptosis, respectively. The results were evaluated by one-way ANOVA with the post hoc multiple comparisons Tukey test and linear trend analysis for shifts in protein expression from Vehicle to 2,4-D, to 2,4,5-T, to *D* + T treatment.

HNE.—This lipid peroxidation biomarker reflects membrane damage [60] associated with pathophysiological states such as neurotoxicity and neurodegeneration [61-63]. HNE levels progressively increased from Vehicle to 2,4-D or 2,4,5-T to the combined *D* + T Agent Orange herbicidal treatments resulting in significant inter-group differences (Table 3) with higher levels in the 2,4-D and 2,4,5-T treated relative to control, and further significant increases in the *D* + T cultures (Fig. 5A), suggesting additive or synergistic effects of the 2,4-D and 2,4,5-T exposures.

8-OHdG.—Increased levels of 8-OHdG reflect oxidative injury and stress [64] related to RNA [65], mitochondrial DNA [66], and nuclear DNA [67] damage. 8-OHdG levels were significantly elevated by the 24-hour exposure to 2,4-D, 2,4,5-T, or *D* + T relative to control. In addition, the *D* + T-associated levels were significantly elevated relative to 2,4-D, but not 2,4,5-T (Fig. 5B).

Ubiquitin.—This multifunctional small molecule conjugates target proteins for degradation via the ubiquitin-proteasome pathway, and regulates cellular processes such as proliferation, apoptosis, and DNA repair [68]. Oxidative stress leading to cellular damage results in the accumulation of ubiquitinated proteins which impairs protein synthesis, including antioxidant mechanisms [68]. In addition, ubiquitin functions as part of the unfolded protein response, contributing to declines in protein synthesis vis-à-vis ER and oxidative stress [68]. The one-way ANOVA test demonstrated a significant inter-group difference in ubiquitin immunoreactivity, and post-hoc Tukey tests revealed higher levels of ubiquitin in 2,4-D, 2,4,5-T, and *D* + T-exposed cultures relative to control, with the highest levels linked to *D* + T (Fig. 5C), paralleling changes in HNE (Fig. 5A).

Caspase 3.—This proteolytic enzyme, when activated, is a critical mediator of cellular apoptosis in response to extrinsic or intrinsic triggers [69]. Caspase-3 has a major role in activating DNA fragmentation linked to apoptosis in mammalian cells [70]. Like the indices of oxidative injury and DNA damage, Caspase 3 immunoreactivity was significantly altered by Agent Orange herbicidal chemical exposures, such that the levels were similarly elevated by 2,4-D and 2,4,5-T, and further increased by the combined *D* + T exposures (Fig. 5D).

PCNA.—Proliferating cell nuclear antigen has essential roles in DNA replication and repair. One-way ANOVA demonstrated significant inter-group differences for PCNA expression ($p = 0.0146$) and a post hoc linear trend ($r^2 = 0.8043$; $p = 0.0036$). However, post hoc Tukey multiple comparisons demonstrated similar levels of PCNA in the Vehicle Control, 2,4-D, and 2,4,5-T cultures, significantly higher levels in *D* + T relative to Vehicle and 2,4,5-T, and a statistical trend increase relative to 2,4-D (Fig. 5E).

GFAP.—Glial fibrillary acidic protein is an astrocyte-expressing intermediate filament protein that has functional roles in maintaining the glial cell architecture, and supporting neighboring neurons and the integrity of the blood-brain barrier [71]. GFAP increases in response to injury and a broad range of acute and chronic CNS diseases, including neurodegeneration [71]. In this study GFAP immunoreactivity progressively increased from the Vehicle to 2,4-D, to 2,4,5-T, to *D* + T treatment effects, corresponding with the highly statistically significant linear trend analysis result (Table 3). Post hoc Tukey multiple comparisons tests revealed significantly higher GFAP expression following each of the Agent Orange herbicide toxin treatments relative to vehicle, and higher levels in the *D* + T versus 2,4-D and 2,4,5-T (Fig. 5F).

Effects of 2,4-D, 2,4,5-T and D + T on metabolic/mitochondrial function (Table 4 and Fig. 6)

Immunoreactivity to GAPDH and mitochondrial complex proteins I-V were measured by Duplex ELISA with results normalized to RPLPO. The one-way ANOVA tests and post

hoc linear trend analysis results are provided in Table 4. The graphs with significant post hoc Tukey multiple comparisons *p*-values are shown in Fig. 4. Linear trends in protein expression were assessed for the transitions from Vehicle to 2,4-D, to 2,4,5-T, to *D* + T treatments.

GAPDH.—GAPDH is an insulin-regulated enzyme that has a critical role in glucose-regulated energy metabolism [54]. Although its levels were found reduced with CNS neurotoxic or neurodegenerative pathology [72, 73], GAPDH has pleiotropic roles. Oxidative stress can impair its catalytic activity and mediate cellular apoptosis and aging [74], and extra glycolytic effects can boost cellular proliferation, or trigger apoptosis via the release of cytochrome c from mitochondria [74]. One-way ANOVA demonstrated significant inter-group differences in GAPDH expression ($p = 0.0218$). Post hoc Tukey tests demonstrated significantly increased levels of GAPDH in *D* + T relative to vehicle, which likely drove the significant r^2 for linear trend analysis ($p = 0.0035$) (Fig. 6A).

Complex I.—Mitochondrial Complex I is NADH ubiquinone oxidoreductase and the largest multi-subunit complex of the respiratory chain. Complex I contributes substantially to the formation of mitochondrial reactive oxygen species via NADH oxidation [75]. Complex I expression was significantly modulated by treatment with Agent Orange herbicidal chemicals as demonstrated by one-way ANOVA ($p = 0.0029$) and post hoc linear trend analysis ($p = 0.0005$). Tukey multiple comparisons tests demonstrated significantly higher levels of Complex I in 2,4,5-T- and *D* + T-treated relative to vehicle and 2,4-D, but no significant difference between 2,4,5-T and *D* + T (Fig. 6B).

Complex II.—Mitochondrial complex II is succinate dehydrogenase. This electron transport protein oxidizes FADH2, transferring electrons to ubiquinol, which carries electrons to Complex III [76]. Consequently, Complex II is at the crossroads of oxidative phosphorylation and the Krebs tricarboxylic acid cycle and has a major role in generating mitochondrial reactive oxygen species [77]. One-way ANOVA demonstrated no significant inter-group differences in the levels of Complex II (Fig. 6C).

Complex III.—Complex III, also termed coenzyme Q-cytochrome c reductase, shunts electrons across the intermembrane space to cytochrome c, generating reactive oxygen species in the intermembrane space or within the matrix [76]. One-way ANOVA demonstrated significant inter-group differences in Complex III expression, and the post hoc linear trend analysis was significant for higher levels with different Agent Orange herbicidal exposures relative to vehicle ($p = 0.003$). Post hoc Tukey tests demonstrated higher levels of Complex III in 2,4-D, 2,4,5-T, and *D* + T-relative to vehicle-treated cultures, but not compared with each other (Fig. 6D).

Complex IV: Complex IV is cytochrome c oxidase (COX). This is the final oxygen-accepting enzyme in the electron transport chain for generating ATP by oxidative phosphorylation [78]. One-way ANOVA demonstrated significant inter-group differences in Complex IV expression. Linear trend analysis was significant for increasing COX expression from Vehicle to single then double Agent Orange herbicidal exposures ($p =$

0.0007). Post hoc Tukey tests revealed higher levels of Complex IV in the 2,4,5-T- and *D* + T-treated relative to Vehicle and higher levels in *D* + T than 2,4-D (Fig. 6E).

Complex V.—Mitochondrial Complex V is ATP synthase which generates ATP from ADP and inorganic phosphate via the ECT proton electrochemical gradient [79]. There were no significant effects of Agent Orange herbicide exposures on Complex V expression in the FLSCs (Fig. 6F).

Effects of 2,4-D, 2,4,5-T and D + T on biomarkers of AD-type neurodegeneration (Table 5 and Fig. 7)

Tau, pTau, AβPP, Aβ, ChAT, and AChE immunoreactivities were used as molecular indices of AD-type neurodegeneration following exposure to Agent Orange herbicidal toxins. One-way ANOVA tests and post hoc linear trend analysis were statistically significant for all but AChE (Table 5).

Tau.—Tau is a microtubule-binding protein that functions in controlling microtubule assembly and stability, impacting axonal transport and growth cone development [80]. Tau's function and subcellular localization are modulated by phosphorylation [81] and targeted in many neurodegenerative diseases, including AD, frontotemporal lobar degeneration, progressive supranuclear palsy, and corticobasal degeneration [82]. With neurodegeneration, neurotoxicity, or oxidative stress, aberrantly phosphorylated tau proteins can accumulate and form aggregates [83] that get ubiquitinated [84] and drive further oxidative stress within neurons [82], or they could undergo fragmentation leading to reduced expression vis-à-vis synaptic disconnection and cytoskeletal collapse [85]. Tau expression was similarly elevated in the 2,4-D and 2,4,5-T treated relative to vehicle cultures, and further elevated by combined *D* + T treatment (Fig. 7A).

pTau.—The pTau antibody detected the S396 phosphorylated epitope of tau, which corresponds to PHF and is one of the many sites that contributes to tau hyperphosphorylation in AD and other neurodegenerative diseases [86]. Besides neurodegeneration, hypoxic-ischemic injury or oxidative stress can also promote tau phosphorylation via glycogen synthase kinase-3β (GSK-3β) activation, as occurs in AD [87]. The mean levels of pTau (S396-PHF) were significantly elevated by 2,4-D or *D* + T treatment relative to Vehicle. In addition, the difference between Vehicle and 2,4,5-T had a statistical trend effect ($p = 0.06$) (Fig. 7B). Although significant inter-group differences were detected for the calculated pTau/tau ratio, the only significant post hoc Tukey test result was reduced levels in the *D* + T relative to Vehicle ($p < 0.05$; not shown). In contrast to all the other linear trend effects, the slope of the linear trend effect line was negative, reflecting combined effects of sharply increased tau accumulation with the modest increases in pTau (S396).

AβPP.—AβPP is abundantly expressed in many organs throughout the body including the brain [88]. AβPP's normal physiological functions are still under investigation, although evidence suggests roles in intercellular adhesion, neuroprotection, neurotropism, and neuronal migration [89]. However, with increased brain expression as occurs in sporadic

AD [90], AβPP's susceptibility to cleavage leads to excess accumulation of neurotoxic/proneurodegenerative Aβ [89]. Similarly elevated mean levels of AβPP were measured in 2,4-D, 2,4,5-T, and *D* + T treated FLSCs relative to control, but there were no inter-group differences with respect to individual or dual Agent Orange herbicide exposures (Fig. 7C).

Aβ.—Proteolytic cleavage of AβPP, initially by beta-secretase and then gamma-secretase [88] yields C-terminal 40 or 42 amino acid amyloid-beta peptides (Aβ) that aggregate or form oligomers and contribute to AD pathology [88]. Aβ immunoreactivity was significantly elevated in the 2,4-D, 2,4,5-T, and *D*+ T treated FLSCs relative to vehicle, with the highest expression associated with *D* + T, suggesting additive effects of the herbicide toxin exposures (Fig. 7D).

ChAT.—Choline acetyltransferase (ChAT) enzymatically generates acetylcholine, a neurotransmitter that becomes deficient in the early stages of AD and other neurodegenerative diseases [91]. ChAT immunoreactivity was significantly elevated by 2,4-D and *D* + T treatments relative to vehicle. In addition, the levels ChAT were significantly higher than in 2,3,5-T cultures, which did not differ significantly from control (Fig. 7E).

AChE.—Acetylcholinesterase breaks down acetylcholine, terminating cholinergic neurotransmission [92]. In AD, AChE expression is reduced [93-95], but the standard-of-care includes treatment with an acetylcholinesterase inhibitor to preserve the already reduced levels of acetylcholine [92, 94, 96, 97]. One-way ANOVA demonstrated no significant intergroup differences with respect to AChE expression (Fig. 7F).

DISCUSSION

Previously, we showed that 2,4-D and 2,4,5-T, the two co-dominant herbicidal toxins in Agent Orange, cause mitochondrial dysfunction, cell death, increased expression of AβPP, Aβ, pTau, elevated indices of oxidative stress, and altered cholinergic function in cultured immature PNET2 human neuronal cells [39], reminiscent of early molecular pathologic findings in AD. This study extends the effort to delineate mechanistic roles of Agent Orange herbicidal toxin exposures in the pathogenesis of AD-type neurodegeneration by utilizing a model of mature intact brain tissue that includes the full complex array of cell types and tissue sub-structures rather than uniform populations of immature neuronal cells. Importantly, in addition to neuronal pathological changes, the ex vivo frontal lobe slice culture model provided new information about the effects of Agent Orange exposure on oligodendrocytes, astrocytes, myelin, and cerebral microvessels. The approach was designed to better characterize the neuropathological, neurotoxic, and neurodegenerative consequences of Agent Orange toxin exposures in young otherwise healthy brains, as would have been the case for Vietnam War era military personnel. In addition, the results could serve to either validate or refute epidemiological data suggesting increased risks of developing AD and other aging-associated neurodegenerative diseases in military personnel that had Agent Orange herbicide exposures [27, 98]. The 2,4-D+2,4,5-T (*D* + T) combined exposures mimicked the effects of Agent Orange and were intended to assess the impacts of both direct military personnel exposures and civilian population exposures that occurred via decades-long persistence of Agent Orange pollutants in the

environment [99]. The independent 2,4-D and 2,4,5-T exposures have relevance to the ongoing human exposures afforded by the continued widespread inclusion of 2,4-D in herbicide and pesticide agricultural, commercial, and consumer products as potential mediators of neurodegeneration and other health risks [7, 100, 101].

Histopathological studies demonstrated that both 2,4-D and 2,4,5-T caused neuronal injury and degeneration, endothelial cell and vascular wall necrosis, oligodendrocyte loss, and white matter parenchymal damage. However, the 2,4-D and 2,4,5-T effects were distinguished bythe more prominent oligodendrocyte loss, white matter parenchymal degeneration and vascular necrosis with 2,4-D, and greater severities of neuronal degeneration and astrocyte activation with 2,4,5-T. The *D* + T combined exposures had additive or synergistic neuropathological effects on neurons, oligodendrocytes, astrocytes, and vascular structures. The immunohistochemical staining for MOG1 provided convincing evidence of white matter myelin loss/degeneration with the separate and combined treatments, and striking activation of GFAP-positive fibrillary astrocytes in the *D* + T treated relative to 2,4-D, 2,4,5-T, and vehicle-treated cultures, supporting the impression of additive or synergistic effects of the two herbicidal compounds present in Agent Orange. These progressive increases in GFAP were confirmed by similarly significant increases in GFAP immunoreactivity measured by ELISA. These overall results are quite intriguing as they suggest that in the early stages of Agent Orange-mediated neurodegeneration multiple CNS cell types are targeted rather than predominantly or solely neurons. This observation raises questions about the spectrum of neuropathology that may accompany the earliest stages of AD in humans to account for the long-term neurodegenerative changes that impact cortical neurons, white matter parenchyma, oligodendrocytes, and micro-vessels distributed in gray and white matter tissue. Indeed, the overlapping neuropathologies are a common finding in children and teens highly exposed to air pollution, with AD being the predominant pathology starting in infants [102-105].

Along with the histopathological evidence of neurodegeneration, we detected significantly increased cytotoxicity following exposure to 2,4-D or 2,4,5-T. The paradoxically negative results obtained with *D* + T treatments most likely reflect severe cellular injury with loss of membrane integrity combined with depletion of enzyme activity as previously discussed [106]. However, other measures of oxidative damage including HNE (lipid peroxidation), 8-OHdG (DNA/RNA damage), ubiquitin (unfolded protein response), and activated Caspase 3 (proapoptosis) provided evidence of increased cellular pathology following 2,4-D or 2,4,5-T treatments, and further increases with the combined *D* + T exposures. HNE is a major α,β-unsaturated aldehyde product of n-6 fatty acid oxidation and lipid peroxidation end-product. HNE functions as a second messenger of oxidative/electrophilic stress [107] and modulates cell survival/death via ER stress induction and promotes cell death via apoptosis [107]. The 2,4-D-, 2,4,5-T-, and *D* + T-induced increases in HNE suggest a role for lipid peroxidation as a mediator of oxidative stress, DNA damage, and activated Caspase-3-associated apoptosis. Likewise, the increased ubiquitin immunoreactivity likely reflects the accumulation of ubiquitin-conjugated proteins targeted for degradation following oxidative damage. These effects of 2.4-D, 2,4,5-T, and *D* + T correspond with the known molecular mediators of AD and other neurodegenerative diseases [82, 108, 109]. Corresponding with the expected responses to injury in the brain, GFAP immunoreactivity increased in parallel

with the indices of oxidative stress and damage, peaking with the *D* + T treatments and mirroring the findings by immunohistochemical staining. In contrast, the PCNA marker of cellular proliferation was similarly expressed in control, 2,4-D, and 2,4,5-T cultures. The selective increase in PCNA following *D* + T most likely reflects a consequence of reactive oxygen species-induced cellular proliferation via oxidative stimulation of mitogenic pathways known to occur with neurodegeneration [110].

The levels of immunoreactivity to mitochondrial complex proteins I-V served as indices of mitochondrial function. Complexes I, III, and IV were significantly modulated by 2,4-D, 2,4,5-T, or *D* + T exposures with predominantly increased expression relative to control. The similarly increased levels of Complex I and IV in the 2,4,5-T and *D* + T suggest that 2,4,5-T was the main driver of NADH (ubiquinone oxidoreductase) and cytochrome c oxidase activity without additive or synergistic effects of 2,4-D, which had no detectable effect on these mitochondrial enzymes. Complex III's similarly elevated levels in the 2,4-D, 2,4,5-T, and *D* + T FLSCs suggest saturated responses to the oxidative injury resulting in the comparable generation of ROS within the matrix. Although these findings appear to conflict with our earlier observation that 2,4-D and 2,4,5-T inhibited MTT activity in immature CNS neuronal cells [39], the disparate results could be attributed to differences in the culture properties, i.e. proliferating versus post-mitotic, neuronal versus mixed cell types in the brain, and monolayer versus tissue slices. Furthermore, the MTT assay reports combined effects of cell viability, proliferation, and mitochondrial function [111, 112] whereas the mitochondrial complex ELISA results corresponded to enzyme protein expression rather than activity per se. Certainly, the increased levels of Complexes I, III, and IV would have led to increased superoxide and ROS generation with attendant damage to lipids, proteins, and nucleic acids [113], corresponding with results shown in Fig. 3. However, at the relatively early stage of tissue analysis post-herbicidal toxin exposure, no significant effects on ATP synthase expression were detected, suggesting that overall oxidative energy had not yet been impaired. The caveat in this interpretation is that the results reflect averaged responses of mixed brain cell types, some of which may have been activated, e.g. astrocytes and microglia, and others inhibited, e.g., neurons.

Tau is a major microtubule-associated binding protein with important roles in maintaining the neuronal cytoarchitecture and inter-neuronal connections [80]. The neuronal cytoskeleton is highly vulnerable to oxidative injury and its degradation, the consequences of which cause growth cone collapse and synaptic disconnection [114, 115]. In AD and other neurodegenerative diseases, hyperphosphorylation of tau on Ser and Thr residues has been linked to stress-mediated increases in the activities of various kinases such as glycogen synthase kinase-3β (GSK-3β) [87], cyclin dependent kinase 5 (Cdk5) [87, 116], and calmodulin-dependent protein kinase (CaMKII) [115], leading to misfolding, aggregation, and intracellular accumulation of tau. The studies herein showed that both tau and pTau were significantly increased in the 2,4-D and *D* + T-treated cultures, and that tau was increased in 2,4,5-T-treated cultures relative to Vehicle. The increases in tau protein were likely mediated by oxidative stress, cytoskeletal collapse, protein aggregation, and possibly ubiquitination. The significantly increased PHF-pTau appeared to be driven by 2,4-D since the levels associated with single and *D* + T dual exposures were similarly elevated. The finding of increased pTau in 2,4-D-treated cultures corresponds with previous observations

in PNET2 CNS neuronal cells [39] and supports the argument that Agent Orange herbicide toxin exposures can promote stress-related tau phosphorylation as in AD.

This study detected elevated AβPP and Aβ in FLSC brain tissue treated with 2,4-D, 2,4,5-T, or *D* + T. The effects of 2,4-D, 2,4,5-T, and *D* + T on AβPP were similar, but they were most pronounced for Aβ following dual *D* + T compared with the single treatments. Previous studies showed that AβPP expression and Aβ immunoreactivity increase with oxidative stress [85] and that AβPP expression is elevated in brains with sporadic AD [95, 117], i.e., unrelated to germline mutations or the *APOE4* genotype. Presumably, the oxidative stress-driven increases in AβPP expression and processing led to the Aβ cleavage product accumulation. Together, these results support the concept that Agent Orange herbicide toxins exert oxidative injury accompanied by AβPP and Aβ-related molecular pathologies that occur in AD-type neurodegeneration.

ChAT is needed for acetylcholine biosynthesis and a specific marker of cholinergic neuron function [118]. In AD, reduced ChAT expression is linked to cognitive impairment [91], and dysregulated insulin signaling in neurons [44, 117, 119, 120]. However, in the very early stages of neurodegeneration manifested by mild cognitive impairment, ChAT is paradoxically increased [121], suggesting a compensatory response to evolving cholinergic pathway failure. The significantly elevated levels of ChAT associated with 2,4-D and *D* + T likely reflect increased efforts to generate acetylcholine in Agent Orange herbicide toxin-stressed cells and appear reminiscent of very early-stage AD.

AChE, has dual roles in regulating hydrolytic metabolism [122, 123], and non-enzymatic functions mediating axonal growth, synaptogenesis, neuronal migration, and cell adhesion [123]. Previous studies demonstrated AD-associated increases in AChE associated with senile plaques [122], and reduced expression in plaque-free regions [93] or in brains that had been subjected to chronic ethanol exposure [53, 124, 125]. The inhibition of AChE can have neurotoxic effects caused by prolonged cholinergic stimulation. Of note is that AChE is a specific target of organophosphates and carbamate pesticides which inhibit enzyme activity [123]. In contrast to the previous finding of AChE inhibition by 2,4-D and 2,4,5-T in CNS neuronal cultures [39], AChE expression in the FLSCs was not significantly modulated by exposure to the Agent Orange herbicide toxins, perhaps due to averaged results from mixed cell populations. Nonetheless, the findings suggest that ChAT activity was dysregulated since the increased expression/activity was incompletely opposed by correspondingly increased AChE expression.

Conclusions

Agent Orange pollutants remain in the environment for decades [99]. Besides the increased risk of generating TCDD with the manufacture of 2,4-D and 2,4,5-T, strong evidence that 2,4,5-T itself causes harm led to its discontinued registered use in the US. Unfortunately, human exposures to 2,4-D still adversely impact global populations due to its widespread inclusion in herbicide and pesticide products, including in the US. The results of these studies using mature brain tissue suggest that Agent Orange damages the CNS in ways that typically occur in neurodegenerative diseases [126-128], and therefore could account for the suspected increased risk of AD and other neurodegenerative diseases

among Vietnam War Veterans. Retrospective epidemiologic [27, 129] and biomarker [98] studies have highlighted the potential contributions of Agent Orange exposures to brain atrophy and neurodegeneration [130], including Parkinson's disease and other forms of neurodegeneration in humans [5, 19, 20, 27, 28]. Differences in the nature/subtype of neurodegeneration following Agent Orange exposures may be attributable to variability in the concurrent presence of other herbicidal toxins in the environment such as TCDD [20, 99, 131] Although the doses of 2,4-D and 2,4,5-T used in these studies correspond with previous reports [38, 47-49], they may have been higher than the levels incorporated into the Agent Orange herbicide sprays [50]. On the other hand, repeated exposures, long intervals of post-exposure follow-up, and persistence of chemicals in the environment and body are concerning for their likely significant impact on the development of Agent Orange-related diseases.

An important limitation of this study pertains to its ex vivo design therefore lack of data pertaining to the long-term and delayed CNS effects of Agent Orange exposure. Another drawback was that the slice cultures, despite their many advantages, are very delicate and fragile, rendering them fragmentable and difficult to evaluate using in situ quantitative approaches. Therefore, the histologic studies served as qualitative tools for reinforcing results obtained with more quantitative approaches such as ELISAs. Finally, the limited experimental tissue obtained constrained the number and nature of experimental assays needed for mechanistic studies such as signal transduction pathway analysis. Nonetheless, the combined descriptive qualitative and quantitative results are sufficiently encouraging to extend the investigations utilizing *in vivo* models and possibly human postmortem brain tissues.

Despite growing appreciation of the broad toxic and carcinogenic effects of 2,4-D, concern has not achieved a level sufficient for federal agencies to ban its use [132]. Currently, the widespread, uncontrolled use of 2,4-D in herbicide and pesticide products is such that one in three Americans has biomarker evidence of prior exposure [133]. The results of the present study and another recent publication [39] support the notion that 2,4-D, 2,4,5-T, and *D* + T (Agent Orange) exert alarming adverse effects on the mature brain/CNS and cause neuropathologic and molecular abnormalities reminiscent of AD as well as other forms of neurodegeneration including motor neuron disease/ALS [7, 134] and Parkinsonism [27, 28]. Additional studies are needed to further characterize Agent Orange herbicide toxin-mediated neurodegeneration in relation to insulin resistance, which is a feature of diabetes mellitus and AD-type neurodegeneration [1, 135].

ACKNOWLEDGMENTS

The authors wish to acknowledge the technical support of Busra Delikkaya for her participation in the early stages of the experiment.

FUNDING

This research was supported by R01AA011431 (SMD) and R01AA028408 (SMD) from the National Institute on Alcohol Abuse and Alcoholism at the National Institutes of Health.

DATA AVAILABILITY

The data supporting the findings of this study are available on request from the corresponding author.

REFERENCES

[1]. de la Monte SM (2017) Insulin resistance and neurodegeneration: Progress towards the development of new therapeutics for Alzheimer's disease. Drugs 77, 47–65. [PubMed: 27988872]

[2]. de la Monte SM, Kril JJ (2014) Human alcohol-related neuropathology. Acta Neuropathol 127, 71–90. [PubMed: 24370929]

[3]. Li X, Yin J, Cheng CM, Sun JL, Li Z, Wu YL (2005) Paraquat induces selective dopaminergic nigrostriatal degeneration in aging C57BL/6 mice. Chin Med J (Engl) 118, 1357–1361. [PubMed: 16157030]

[4]. Hsieh YC, Mounsey RB, Teismann P (2011) MPP(+)-induced toxicity in the presence of dopamine is mediated by COX-2 through oxidative stress. Naunyn Schmiedebergs Arch Pharmacol 384, 157–167. [PubMed: 21667279]

[5]. McKnight S, Hack N (2020) Toxin-induced parkinsonism. Neurol Clin 38, 853–865. [PubMed: 33040865]

[6]. Fahim MA, Shehab S, Nemmar A, Adem A, Dhanasekaran S, Hasan MY (2013) Daily subacute paraquat exposure decreases muscle function and substantia nigra dopamine level. Physiol Res 62, 313–321. [PubMed: 23489189]

[7]. Andrew A, Zhou J, Gui J, Harrison A, Shi X, Li M, Guetti B, Nathan R, Tischbein M, Pioro EP, Stommel E, Bradley W (2021) Pesticides applied to crops and amyotrophic lateral sclerosis risk in the U.S. Neurotoxicology 87, 128–135. [PubMed: 34562505]

[8]. Kamel F, Umbach DM, Bedlack RS, Richards M, Watson M, Alavanja MC, Blair A, Hoppin JA, Schmidt S, Sandler DP (2012) Pesticide exposure and amyotrophic lateral sclerosis. Neurotoxicology 33, 457–462. [PubMed: 22521219]

[9]. Spencer P, Fry RC, Kisby GE (2012) Unraveling 50-year-old clues linking neurodegeneration and cancer to cycad toxins: Are microRNAs common mediators? Front Genet 3, 192. [PubMed: 23060898]

[10]. Spencer PS, Palmer VS, Kisby GE (2020) Western Pacific ALS-PDC: Evidence implicating cycad genotoxins. J Neurol Sci 419, 117185. [PubMed: 33190068]

[11]. de la Monte SM, Neusner A, Chu J, Lawton M (2009) Epidemilogical trends strongly suggest exposures as etiologic agents in the pathogenesis of sporadic Alzheimer's disease, diabetes mellitus, and non-alcoholic steatohepatitis. J Alzheimers Dis 17, 519–529. [PubMed: 19363256]

[12]. Bryan NS, Alexander DD, Coughlin JR, Milkowski AL, Boffetta P (2012) Ingested nitrate and nitrite and stomach cancer risk: An updated review. Food Chem Toxicol 50, 3646–3665. [PubMed: 22889895]

[13]. Brunnemann KD, Hecht SS, Hoffmann D (1982) N-nitrosamines: Environmental occurrence, *in vivo* formation and metabolism. J Toxicol Clin Toxicol 19, 661–688. [PubMed: 6761448]

[14]. de la Monte SM, Tong M, Lawton M, Longato L (2009) Nitrosamine exposure exacerbates high fat diet-mediated type 2 diabetes mellitus, non-alcoholic steatohepatitis, and neurodegeneration with cognitive impairment. Mol Neurodegener 4, 54. [PubMed: 20034403]

[15]. de la Monte SM, Tong M (2009) Mechanisms of nitrosamine-mediated neurodegeneration: Potential relevance to sporadic Alzheimer's disease. J Alzheimers Dis 17, 817–825. [PubMed: 19542621]

[16]. Thomas TL, Kang HK (1990) Mortality and morbidity among Army Chemical Corps Vietnam veterans: A preliminary report. Am J Ind Med 18, 665–673. [PubMed: 2264565]

[17]. Institute of Medicine (US) Committee to review the health effects in Vietnam veterans of exposure to herbicides (Third Biennial Update) (2001) Veterans and Agent Orange: Update 2000, National Academies Press (US), Washington (DC).

[18]. Ambrus JL, Islam A, Akhter S, Dembinski W, Kulaylat M, Ambrus CM (2004) Multiple medical problems following agent orange exposure. J Med 35, 265–269. [PubMed: 18084883]

[19]. Yi SW, Hong JS, Ohrr H, Yi JJ (2014) Agent Orange exposure and disease prevalence in Korean Vietnam veterans: The Korean veterans health study. Environ Res 133, 56–65. [PubMed: 24906069]

[20]. Institute of Medicine (1994) Veterans and Agent Orange: Health Effects of Herbicides Used in Vietnam, The National Academies Press, Washington (DC).

[21]. Le TN, Johansson A (2001) Impact of chemical warfare with agent orange on women's reproductive lives in Vietnam: A pilot study. Reprod Health Matters 9, 156–164. [PubMed: 11765392]

[22]. Ngo AD, Taylor R, Roberts CL, Nguyen TV (2006) Association between Agent Orange and birth defects: Systematic review and meta-analysis. Int J Epidemiol 35, 1220–1230. [PubMed: 16543362]

[23]. Stellman SD, Stellman JM, Sommer JF, Jr. (1988) Health and reproductive outcomes among American Legionnaires in relation to combat and herbicide exposure in Vietnam. Environ Res 47, 150–174. [PubMed: 3263269]

[24]. Wolfe WH, Michalek JE, Miner JC, Rahe A, Silva J, Thomas WF, Grubbs WD, Lustik MB, Karrison TG, Roegner RH, Williams DE (1990) Health status of Air Force veterans occupationally exposed to herbicides in Vietnam. I. Physical health. JAMA 264, 1824–1831. [PubMed: 2402041]

[25]. Henriksen GL, Ketchum NS, Michalek JE, Swaby JA (1997) Serum dioxin and diabetes mellitus in veterans of Operation Ranch Hand. Epidemiology 8, 252–258. [PubMed: 9115019]

[26]. Michalek JE, Ketchum NS, Akhtar FZ (1998) Postservice mortality of US Air Force veterans occupationally exposed to herbicides in Vietnam: 15-year follow-up. Am J Epidemiol 148, 786–792. [PubMed: 9786233]

[27]. de la Monte SM, Goel A (2022) Agent Orange reviewed: Potential role in peripheral neuropathy and neurodegeneration. J Mil Veterans Health 30, 17–26. [PubMed: 36785586]

[28]. Martinez S, Yaffe K, Li Y, Byers AL, Peltz CB, Barnes DE (2021) Agent Orange exposure and dementia diagnosis in US Veterans of the Vietnam Era. JAMA Neurol 78, 473–477. [PubMed: 33492338]

[29]. Kim JS, Lim HS, Cho SI, Cheong HK, Lim MK (2003) Impact of Agent Orange exposure among Korean Vietnam veterans. Ind Health 41, 149–157. [PubMed: 12916744]

[30]. Michalek JE, Akhtar FZ, Arezzo JC, Garabrant DH, Albers JW (2001) Serum dioxin and peripheral neuropathy in veterans of Operation Ranch Hand. Neurotoxicology 22, 479–490. [PubMed: 11577805]

[31]. Yi SW, Ohrr H, Hong JS, Yi JJ (2013) Agent Orange exposure and prevalence of self-reported diseases in Korean Vietnam veterans. J Prev Med Public Health 46, 213–225. [PubMed: 24137524]

[32]. Gervais J, Luukinen B, Buhl K, Stone D (2008) 2,4-D Technical Fact Sheet. National Pesticide Information Center, Oregon State University Extension Services. http://npic.orst.edu/factsheets/archive/2,4-DTech.html.

[33]. NEPIS (1988) 2,4,5-trichlorophenoxyacetic Acid Health Advisory, Office Of Drinking Water U S Environmental Protection Agency. U.S. Environmental Protection Agency, pp. 1–25. https://nepis.epa.gov/Exe/ZyPURL.cgi?Dockey=2000SPAO.txt

[34]. Bortolozzi AA, Duffard RO, Evangelista de Duffard AM (1999) Behavioral alterations induced in rats by a pre- and postnatal exposure to 2,4-dichlorophenoxyacetic acid. Neurotoxicol Teratol 21, 451–465. [PubMed: 10440489]

[35]. Duffard R, Garcia G, Rosso S, Bortolozzi A, Madariaga M, di Paolo O, Evangelista de Duffard AM (1996) Central nervous system myelin deficit in rats exposed to 2,4-dichlorophenoxyacetic acid throughout lactation. Neurotoxicol Teratol 18, 691–696. [PubMed: 8947946]

[36]. Oliveira GH, Palermo-Neto J (1993) Effects of 2,4-dichlorophenoxyacetic acid (2,4-D) on open-field behaviour and neurochemical parameters of rats. Pharmacol Toxicol 73, 79–85. [PubMed: 7504253]

[37]. Rosso SB, Di Paolo OA, Evangelista de Duffard AM, Duffard R (1997) Effects of 2,4-dichlorophenoxyacetic acid on central nervous system of developmental rats. Associated changes in ganglioside pattern. Brain Res 769, 163–167. [PubMed: 9374285]

[38]. Sharifi Pasandi M, Hosseini Shirazi F, Gholami MR, Salehi H, Najafzadeh N, Mazani M, Ghasemi Hamidabadi H, Niapour A (2017) Epi/perineural and Schwann cells as well as perineural sheath integrity are affected following 2,4-D exposure. Neurotox Res 32, 624–638. [PubMed: 28699141]

[39]. de la Monte SM, Goel A, Tong M, Delikkaya B (2023) Agent Orange causes metabolic dysfunction and molecular pathology reminiscent of Alzheimer's disease. J Alzheimers Dis Rep 7, 751–766. [PubMed: 37662613]

[40]. Sohrabi T, Mirzaei-Behbahani B, Zadali R, Pirhaghi M, Morozova-Roche LA, Meratan AA (2023) Common mechanisms underlying alpha-synuclein-induced mitochondrial dysfunction in Parkinson's disease. J Mol Biol 435, 167992. [PubMed: 36736886]

[41]. Argueti-Ostrovsky S, Alfahel L, Kahn J, Israelson A (2021) All roads lead to Rome: Different molecular players converge to common toxic pathways in neurodegeneration. Cells 10, 2438. [PubMed: 34572087]

[42]. Trigo D, Avelar C, Fernandes M, Sa J, da Cruz ESO (2022) Mitochondria, energy, and metabolism in neuronal health and disease. FEBS Lett 596, 1095–1110. [PubMed: 35088449]

[43]. Upadhayay S, Yedke NG, Rahi V, Singh S, Kumar S, Arora A, Chandolia P, Kaur P, Kumar M, Koshal P, Jamwal S, Kumar P (2023) An overview of the pathophysiological mechanisms of 3-nitropropionic acid (3-NPA) as a neurotoxin in a Huntington's disease model and its relevance to drug discovery and development. Neurochem Res 48, 1631–1647. [PubMed: 36738367]

[44]. Le T, Tong M, Nguyen V, de la Monte SM (2013) PPAR agonist rescue of ethanol-impaired brain insulin signaling: Cerebellar slice culture model. J Drug Alcohol Res 2, 235611.

[45]. Reich D, Gallucci G, Tong M, de la Monte SM (2018) Therapeutic advantages of dual targeting of PPAR-delta and PPAR-gamma in an experimental model of sporadic Alzheimer's disease. J Parkinsons Dis Alzheimers Dis 5, 10.13188/2376-922X.1000025.

[46]. Tong M, Deochand C, Didsbury J, de la Monte SM (2016) T3D-959: A multi-faceted disease remedial drug candidate for the treatment of Alzheimer's disease. J Alzheimers Dis 51, 123–138. [PubMed: 26836193]

[47]. Soloneski S, Gonzalez NV, Reigosa MA, Larramendy ML (2007) Herbicide 2,4-dichlorophenoxyacetic acid (2,4-D)-induced cytogenetic damage in human lymphocytes *in vitro* in presence of erythrocytes. Cell Biol Int 31, 1316–1322. [PubMed: 17606385]

[48]. Bertheussen K, Yousef MI, Figenschau Y (1997) A new sensitive cell culture test for the assessment of pesticide toxicity. J Environ Sci Health B 32, 195–211. [PubMed: 9090862]

[49]. Gonzalez M, Soloneski S, Reigosa MA, Larramendy ML (2005) Genotoxicity of the herbicide 2,4-dichlorophenoxyacetic and a commercial formulation, 2,4-dichlorophenoxyacetic acid dimethylamine salt. I. Evaluation of DNA damage and cytogenetic endpoints in Chinese Hamster ovary (CHO) cells. Toxicol In Vitro 19, 289–297. [PubMed: 15649642]

[50]. Basrur SV, Fletcher RA, Basrur PK (1976) In vitro effects of 2,4-dichlorophenoxy acetic acid (2,4-D) on bovine cells. Can J Comp Med 40, 408–415. [PubMed: 1000402]

[51]. Tong M, Ziplow JL, Mark P, de la Monte SM (2022) Dietary soy prevents alcohol-mediated neurocognitive dysfunction and associated impairments in brain insulin pathway signaling in an adolescent rat model. Biomolecules 12, 676. [PubMed: 35625605]

[52]. Lester-Coll N, Rivera EJ, Soscia SJ, Doiron K, Wands JR, de la Monte SM (2006) Intracerebral streptozotocin model of type 3 diabetes: Relevance to sporadic Alzheimer's disease. J Alzheimers Dis 9, 13–33. [PubMed: 16627931]

[53]. Tong M, Yu R, Deochand C, de la Monte SM (2015) Differential contributions of alcohol and the nicotine-derived nitrosamine ketone (NNK) to insulin and insulin-like growth factor resistance in the adolescent rat brain. Alcohol Alcohol 50, 670–679. [PubMed: 26373814]

[54]. Alexander BM, Dugast I, Ercolani L, Kong XF, Giere L, Nasrin N (1992) Multiple insulin-responsive elements regulate transcription of the GAPDH gene. Adv Enzyme Regul 32, 149–159. [PubMed: 1386708]

[55]. DaDalt AA, Bonham CA, Lotze GP, Luiso AA, Vacratsis PO (2022) Src-mediated phosphorylation of the ribosome biogenesis factor hYVH1 affects its localization, promoting partitioning to the 60S ribosomal subunit. J Biol Chem 298, 102679. [PubMed: 36370849]

[56]. de la Monte SM, Tong M, Carlson RI, Carter JJ, Longato L, Silbermann E, Wands JR (2009) Ethanol inhibition of aspartyl-asparaginyl-beta-hydroxylase in fetal alcohol spectrum disorder: Potential link to the impairments in central nervous system neuronal migration. Alcohol 43, 225–240. [PubMed: 19393862]

[57]. Liu HT, Zou YX, Zhu WJ, Sen L, Zhang GH, Ma RR, Guo XY, Gao P (2022) lncRNA THAP7-AS1, transcriptionally activated by SP1 and post-transcriptionally stabilized by METTL3-mediated m6A modification, exerts oncogenic properties by improving CUL4B entry into the nucleus. Cell Death Differ 29, 627–641. [PubMed: 34608273]

[58]. Xie JJ, Jiang YY, Jiang Y, Li CQ, Lim MC, An O, Mayakonda A, Ding LW, Long L, Sun C, Lin LH, Chen L, Wu JY, Wu ZY, Cao Q, Fang WK, Yang W, Soukiasian H, Meltzer SJ, Yang H, Fullwood M, Xu LY, Li EM, Lin DC, Koeffler HP (2018) Super-enhancer-driven long non-coding RNA LINC01503, regulated by TP63, is over-expressed and oncogenic in squamous cell carcinoma. Gastroenterology 154, 2137–2151 e2131. [PubMed: 29454790]

[59]. Tong M, Gonzalez-Navarrete H, Kirchberg T, Gotama B, Yalcin EB, Kay J, de la Monte SM (2017) Ethanol-induced white matter atrophy is associated with impaired expression of aspartyl-asparaginyl-beta-hydroxylase (ASPH) and Notch signaling in an experimental rat model. J Drug Alcohol Res 6, 236033. [PubMed: 29204305]

[60]. Ayala A, Munoz MF, Arguelles S (2014) Lipid peroxidation: Production, metabolism, and signaling mechanisms of malondialdehyde and 4-hydroxy-2-nonenal. Oxid Med Cell Longev 2014, 360438. [PubMed: 24999379]

[61]. Tong M, Dong M, de la Monte SM (2009) Brain insulin-like growth factor and neurotrophin resistance in Parkinson's disease and dementia with Lewy bodies: Potential role of manganese neurotoxicity. J Alzheimers Dis 16, 585–599. [PubMed: 19276553]

[62]. Moon KH, Tajuddin N, Brown J 3rd, Neafsey EJ, Kim HY, Collins MA (2014) Phospholipase A2, oxidative stress, and neurodegeneration in binge ethanol-treated organotypic slice cultures of developing rat brain. Alcohol Clin Exp Res 38, 161–169. [PubMed: 23909864]

[63]. Liou CJ, Tong M, Vonsattel JP, de la Monte SM (2019) Altered brain expression of insulin and insulin-like growth factors in frontotemporal lobar degeneration: Another degenerative disease linked to dysregulation of insulin metabolic pathways. ASN Neuro 11, 1759091419839515.

[64]. Omari Shekaftik S, Nasirzadeh N (2021) 8-Hydroxy-2'-deoxyguanosine (8-OHdG) as a biomarker of oxidative DNA damage induced by occupational exposure to nanomaterials: A systematic review. Nanotoxicology 15, 850–864. [PubMed: 34171202]

[65]. Cattley RC, Glover SE (1993) Elevated 8-hydroxydeoxyguanosine in hepatic DNA of rats following exposure to peroxisome proliferators: Relationship to carcinogenesis and nuclear localization. Carcinogenesis 14, 2495–2499. [PubMed: 8269617]

[66]. Torres-Gonzalez M, Gawlowski T, Kocalis H, Scott BT, Dillmann WH (2014) Mitochondrial 8-oxoguanine glycosylase decreases mitochondrial fragmentation and improves mitochondrial function in H9C2 cells under oxidative stress conditions. Am J Physiol Cell Physiol 306, C221–229. [PubMed: 24304833]

[67]. Qing X, Shi D, Lv X, Wang B, Chen S, Shao Z (2019) Prognostic significance of 8-hydroxy-2'-deoxyguanosine in solid tumors: A meta-analysis. BMC Cancer 19, 997. [PubMed: 31651287]

[68]. Dougherty SE, Maduka AO, Inada T, Silva GM (2020) Expanding role of ubiquitin in translational control. Int J Mol Sci 21, 1151. [PubMed: 32050486]

[69]. Porter AG, Janicke RU (1999) Emerging roles of caspase-3 in apoptosis. Cell Death Differ 6, 99–104. [PubMed: 10200555]

[70]. Wolf BB, Schuler M, Echeverri F, Green DR (1999) Caspase-3 is the primary activator of apoptotic DNA fragmentation via DNA fragmentation factor-45/inhibitor of caspase-activated DNase inactivation. J Biol Chem 274, 30651–30656. [PubMed: 10521451]

[71]. McKeon A, Benarroch EE (2018) Glial fibrillary acid protein: Functions and involvement in disease. Neurology 90, 925–930. [PubMed: 29653988]

[72]. de la Monte SM, Tong M, Bowling N, Moskal P (2011) si-RNA inhibition of brain insulin or insulin-like growth factor receptors causes developmental cerebellar abnormalities: Relevance to fetal alcohol spectrum disorder. Mol Brain 4, 13. [PubMed: 21443795]

[73]. de la Monte SM, Wands JR (2002) Chronic gestational exposure to ethanol impairs insulin-stimulated survival and mitochondrial function in cerebellar neurons. Cell Mol Life Sci 59, 882–893. [PubMed: 12088287]

[74]. Nicholls C, Li H, Liu JP (2012) GAPDH: A common enzyme with uncommon functions. Clin Exp Pharmacol Physiol 39, 674–679. [PubMed: 21895736]

[75]. Wirth C, Brandt U, Hunte C, Zickermann V (2016) Structure and function of mitochondrial complex I. Biochim Biophys Acta 1857, 902–914. [PubMed: 26921811]

[76]. Chandel NS (2010) Mitochondrial complex III: An essential component of universal oxygen sensing machinery? Respir Physiol Neurobiol 174, 175–181. [PubMed: 20708106]

[77]. Bezawork-Geleta A, Rohlena J, Dong L, Pacak K, Neuzil J (2017) Mitochondrial complex II: At the crossroads. Trends Biochem Sci 42, 312–325. [PubMed: 28185716]

[78]. Kadenbach B (2021) Complex IV - The regulatory center of mitochondrial oxidative phosphorylation. Mitochondrion 58, 296–302. [PubMed: 33069909]

[79]. Jonckheere AI, Smeitink JA, Rodenburg RJ (2012) Mitochondrial ATP synthase: Architecture, function and pathology. J Inherit Metab Dis 35, 211–225. [PubMed: 21874297]

[80]. Hamm M, Bailey R, Shaw G, Yen SH, Lewis J, Giasson BI (2015) Physiologically relevant factors influence tau phosphorylation by leucine-rich repeat kinase 2. J Neurosci Res 93, 1567–1580. [PubMed: 26123245]

[81]. Wegmann S, Biernat J, Mandelkow E (2021) A current view on tau protein phosphorylation in Alzheimer's disease. Curr Opin Neurobiol 69, 131–138. [PubMed: 33892381]

[82]. Orr ME, Sullivan AC, Frost B (2017) A brief overview of tauopathy: Causes, consequences, and therapeutic strategies. Trends Pharmacol Sci 38, 637–648. [PubMed: 28455089]

[83]. Despres C, Byrne C, Qi H, Cantrelle FX, Huvent I, Chambraud B, Baulieu EE, Jacquot Y, Landrieu I, Lippens G, Smet-Nocca C (2017) Identification of the tau phosphorylation pattern that drives its aggregation. Proc Natl Acad Sci U S A 114, 9080–9085. [PubMed: 28784767]

[84]. Li L, Jiang Y, Wang JZ, Liu R, Wang X (2021) Tau ubiquitination in Alzheimer's disease. Front Neurol 12, 786353. [PubMed: 35211074]

[85]. Chen GJ, Xu J, Lahousse SA, Caggiano NL, de la Monte SM (2003) Transient hypoxia causes Alzheimer-type molecular and biochemical abnormalities in cortical neurons: Potential strategies for neuroprotection. J Alzheimers Dis 5, 209–228. [PubMed: 12897406]

[86]. Miao J, Shi R, Li L, Chen F, Zhou Y, Tung YC, Hu W, Gong CX, Iqbal K, Liu F (2019) Pathological tau from Alzheimer's brain induces site-specific hyperphosphorylation and SDS- and reducing agent-resistant aggregation of tau *in vivo*. Front Aging Neurosci 11, 34. [PubMed: 30890929]

[87]. Lovestone S, Reynolds CH, Latimer D, Davis DR, Anderton BH, Gallo JM, Hanger D, Mulot S, Marquardt B, Stabel S, Woodgett JR, Miller CCJ (1994) Alzheimer's disease-like phosphorylation of the microtubule-associated protein tau by glycogen synthase kinase-3 in transfected mammalian cells. Curr Biol 4, 1077–1086. [PubMed: 7704571]

[88]. Evin G, Weidemann A (2002) Biogenesis and metabolism of Alzheimer's disease Abeta amyloid peptides. Peptides 23, 1285–1297. [PubMed: 12128085]

[89]. Hiltunen M, van Groen T, Jolkkonen J (2009) Functional roles of amyloid-beta protein precursor and amyloid-beta peptides: Evidence from experimental studies. J Alzheimers Dis 18, 401–412. [PubMed: 19584429]

[90]. de la Monte SM (2012) Contributions of brain insulin resistance and deficiency in amyloid-related neurodegeneration in Alzheimer's disease. Drugs 72, 49–66. [PubMed: 22191795]

[91]. Ikonomovic MD, Mufson EJ, Wuu J, Bennett DA, DeKosky ST (2005) Reduction of choline acetyltransferase activity in primary visual cortex in mild to moderate Alzheimer's disease. Arch Neurol 62, 425–430. [PubMed: 15767507]

[92]. Trang A, Khandhar PB (2023) Physiology, acetylcholinesterase. In StatPearls, StatPearls Publishing, Treasure Island (FL), pp. 1–4.

[93]. Kish SJ, Schut L, Simmons J, Gilbert J, Chang LJ, Rebbetoy M (1988) Brain acetylcholinesterase activity is markedly reduced in dominantly-inherited olivopontocerebellar atrophy. J Neurol Neurosurg Psychiatry 51, 544–548. [PubMed: 3164041]

[94]. Meena VK, Chaturvedi S, Sharma RK, Mishra AK, Hazari PP (2019) Potent acetylcholinesterase selective and reversible homodimeric agent based on tacrine for theranostics. Mol Pharm 16, 2296–2308. [PubMed: 31059278]

[95]. Steen E, Terry BM, Rivera EJ, Cannon JL, Neely TR, Tavares R, Xu XJ, Wands JR, de la Monte SM (2005) Impaired insulin and insulin-like growth factor expression and signaling mechanisms in Alzheimer's disease–is this type 3 diabetes? J Alzheimers Dis 7, 63–80. [PubMed: 15750215]

[96]. Hull M, Berger M, Heneka M (2006) Disease-modifying therapies in Alzheimer's disease: How far have we come? Drugs 66, 2075–2093. [PubMed: 17112302]

[97]. Davis RE, Doyle PD, Carroll RT, Emmerling MR, Jaen J (1995) Cholinergic therapies for Alzheimer's disease. Palliative or disease altering? Arzneimittelforschung 45, 425–431. [PubMed: 7763338]

[98]. Yang Y, Giau VV, An SSA, Kim S (2018) Plasma oligomeric beta amyloid in Alzheimer's disease with history of agent orange exposure. Dement Neurocogn Disord 17, 41–49. [PubMed: 30906391]

[99]. Olson KR, Morton LW (2019) Long-term fate of agent orange and dioxin TCDD contaminated soils and sediments in Vietnam hotspots. Open J Soil Sci 09, 1–34.

[100]. Perrin L, Moisan F, Spinosi J, Chaperon L, Jezewski-Serra D, Elbaz A (2023) Combining crop-exposure matrices and land use data to estimate indices of environmental and occupational exposure to pesticides. J Expo Sci Environ Epidemiol, doi: 10.1038/s41370-023-00562-w.

[101]. Rocha VA, Aquino AM, Magosso N, Souza PV, Justulin LA, Domeniconi RF, Barbisan LF, Romualdo GR, Scarano WR (2023) 2,4-Dichlorophenoxyacetic Acid (2,4-D) exposure during postnatal development alters the effects of Western diet on mouse prostate. Reprod Toxicol 120, 108449. [PubMed: 37516258]

[102]. Calderon-Garciduenas L, Gonzalez-Maciel A, Reynoso-Robles R, Delgado-Chavez R, Mukherjee PS, Kulesza RJ, Torres-Jardon R, Avila-Ramirez J, Villarreal-Rios R (2018) Hallmarks of Alzheimer disease are evolving relentlessly in Metropolitan Mexico City infants, children and young adults. APOE4 carriers have higher suicide risk and higher odds of reaching NFT stage V at ≤40 years of age. Environ Res 164, 475–487. [PubMed: 29587223]

[103]. Calderon-Garciduenas L, Stommel EW, Lachmann I, Waniek K, Chao CK, Gonzalez-Maciel A, Garcia-Rojas E, Torres-Jardon R, Delgado-Chavez R, Mukherjee PS (2022) TDP-43 CSF concentrations increase exponentially with age in Metropolitan Mexico City young urbanites highly exposed to PM(2.5) and ultrafine particles and historically showing Alzheimer and Parkinson's hallmarks. Brain TDP-43 pathology in MMC residents is associated with high cisternal CSF TDP-43 concentrations. Toxics 10, 559. [PubMed: 36287840]

[104]. Calderon-Garciduenas L, Gonzalez-Maciel A, Reynoso-Robles R, Silva-Pereyra HG, Torres-Jardon R, Brito-Aguilar R, Ayala A, Stommel EW, Delgado-Chavez R (2022) Environmentally toxic solid nanoparticles in noradrenergic and dopaminergic nuclei and cerebellum of metropolitan Mexico City children and young adults with neural quadruple misfolded protein pathologies and high exposures to nano particulate matter. Toxics 10, 164. [PubMed: 35448425]

[105]. Calderon-Garciduenas L, Ayala A (2022) Air pollution, ultrafine particles, and your brain: Are combustion nanoparticle emissions and engineered nanoparticles causing preventable fatal neurodegenerative diseases and common neuropsychiatric outcomes? Environ Sci Technol 56, 6847–6856. [PubMed: 35193357]

[106]. Cho MH, Niles A, Huang R, Inglese J, Austin CP, Riss T, Xia M (2008) A bioluminescent cytotoxicity assay for assessment of membrane integrity using a proteolytic biomarker. Toxicol In Vitro 22, 1099–1106. [PubMed: 18400464]

[107]. Dalleau S, Baradat M, Gueraud F, Huc L (2013) Cell death and diseases related to oxidative stress: 4-hydroxynonenal (HNE) in the balance. Cell Death Differ 20, 1615–1630. [PubMed: 24096871]

[108]. Olfati N, Shoeibi A, Litvan I (2022) Clinical spectrum of tauopathies. Front Neurol 13, 944806. [PubMed: 35911892]

[109]. Silva MC, Haggarty SJ (2020) Tauopathies: Deciphering disease mechanisms to develop effective therapies. Int J Mol Sci 21, 8948. [PubMed: 33255694]

[110]. Klein JA, Ackerman SL (2003) Oxidative stress, cell cycle, and neurodegeneration. J Clin Invest 111, 785–793. [PubMed: 12639981]

[111]. Morgan DM (1998) Tetrazolium (MTT) assay for cellular viability and activity. Methods Mol Biol 79, 179–183. [PubMed: 9463833]

[112]. Ghasemi M, Turnbull T, Sebastian S, Kempson I (2021) The MTT assay: utility, limitations, pitfalls, and interpretation in bulk and single-cell analysis. Int J Mol Sci 22, 12827. [PubMed: 34884632]

[113]. Guo C, Sun L, Chen X, Zhang D (2013) Oxidative stress, mitochondrial damage and neurodegenerative diseases. Neural Regen Res 8, 2003–2014. [PubMed: 25206509]

[114]. Mandelkow EM, Stamer K, Vogel R, Thies E, Mandelkow E (2003) Clogging of axons by tau, inhibition of axonal traffic and starvation of synapses. Neurobiol Aging 24, 1079–1085. [PubMed: 14643379]

[115]. Kamat PK, Kalani A, Rai S, Swarnkar S, Tota S, Nath C, Tyagi N (2016) Mechanism of oxidative stress and synapse dysfunction in the pathogenesis of Alzheimer's disease: Understanding the therapeutics strategies. Mol Neurobiol 53, 648–661. [PubMed: 25511446]

[116]. Pei JJ, Grundke-Iqbal I, Iqbal K, Bogdanovic N, Winblad B, Cowburn RF (1998) Accumulation of cyclin-dependent kinase 5 (cdk5) in neurons with early stages of Alzheimer's disease neurofibrillary degeneration. Brain Res 797, 267–277. [PubMed: 9666145]

[117]. Rivera EJ, Goldin A, Fulmer N, Tavares R, Wands JR, de la Monte SM (2005) Insulin and insulin-like growth factor expression and function deteriorate with progression of Alzheimer's disease: Link to brain reductions in acetylcholine. J Alzheimers Dis 8, 247–268. [PubMed: 16340083]

[118]. Oda Y (1999) Choline acetyltransferase: The structure, distribution and pathologic changes in the central nervous system. Pathol Int 49, 921–937. [PubMed: 10594838]

[119]. Cohen AC, Tong M, Wands JR, de la Monte SM (2007) Insulin and insulin-like growth factor resistance with neurodegeneration in an adult chronic ethanol exposure model. Alcohol Clin Exp Res 31, 1558–1573. [PubMed: 17645580]

[120]. Soscia SJ, Tong M, Xu XJ, Cohen AC, Chu J, Wands JR, de la Monte SM (2006) Chronic gestational exposure to ethanol causes insulin and IGF resistance and impairs acetylcholine homeostasis in the brain. Cell Mol Life Sci 63, 2039–2056. [PubMed: 16909201]

[121]. DeKosky ST, Ikonomovic MD, Styren SD, Beckett L, Wisniewski S, Bennett DA, Cochran EJ, Kordower JH, Mufson EJ (2002) Upregulation of choline acetyltransferase activity in hippocampus and frontal cortex of elderly subjects with mild cognitive impairment. Ann Neurol 51, 145–155. [PubMed: 11835370]

[122]. Garcia-Ayllon MS, Small DH, Avila J, Saez-Valero J (2011) Revisiting the role of acetylcholinesterase in Alzheimer's disease: Cross-talk with p-tau and beta-amyloid. Front Mol Neurosci 4, 22. [PubMed: 21949503]

[123]. Lionetto MG, Caricato R, Calisi A, Giordano ME, Schettino T (2013) Acetylcholinesterase as a biomarker in environmental and occupational medicine: New insights and future perspectives. Biomed Res Int 2013, 321213. [PubMed: 23936791]

[124]. Pires RG, Pereira SR, Oliveira-Silva IF, Franco GC, Ribeiro AM (2005) Cholinergic parameters and the retrieval of learned and re-learned spatial information: A study using a model of Wernicke-Korsakoff Syndrome. Behav Brain Res 162, 11–21. [PubMed: 15922063]

[125]. Jamal M, Ameno K, Miki T, Wang W, Kumihashi M, Isse T, Kawamoto T, Kitagawa K, Nakayama K, Ijiri I, Kinoshita H (2009) Cholinergic alterations following alcohol exposure in the frontal cortex of Aldh2-deficient mice models. Brain Res 1295, 37–43. [PubMed: 19664611]

[126]. de la Monte SM, Wands JR (2006) Molecular indices of oxidative stress and mitochondrial dysfunction occur early and often progress with severity of Alzheimer's disease. J Alzheimers Dis 9, 167–181. [PubMed: 16873964]

[127]. Friese MA, Schattling B, Fugger L (2014) Mechanisms of neurodegeneration and axonal dysfunction in multiple sclerosis. Nat Rev Neurol 10, 225–238. [PubMed: 24638138]

[128]. Yan MH, Wang X, Zhu X (2013) Mitochondrial defects and oxidative stress in Alzheimer disease and Parkinson disease. Free Radic Biol Med 62, 90–101. [PubMed: 23200807]

[129]. Yang Y, Cheon M, Kwak YT (2016) Is Parkinson's disease with history of agent orange exposure different from idiopathic Parkinson's disease? Dement Neurocogn Disord 15, 75–81. [PubMed: 30906346]

[130]. Lee HA, Kyeong S, Kim DH (2022) Long-term effects of defoliant exposure on brain atrophy progression in humans. Neurotoxicology 92, 25–32. [PubMed: 35830900]

[131]. Mofenson H, Becker C, Kimbrough R, Lawrence R, Lovejoy F, Winters W, Carracio TR, Hardel LK, Rumack BH, Spyker D (1985) Commentary on 2,3,7,8-tetrachlorodibenzo-para-dioxin (TCDD). Vet Hum Toxicol 27, 434–438. [PubMed: 4060565]

[132]. Solomon G, Agent Orange in Your Backyard: The Harmful Pesticide 2,4-D, https://www.theatlantic.com/health/archive/2012/02/agent-orange-in-your-backyard-the-harmful-pesticide-2-4-d/253506/.

[133]. Freisthler MS, Robbins CR, Benbrook CM, Young HA, Haas DM, Winchester PD, Perry MJ (2022) Association between increasing agricultural use of 2,4-D and population biomarkers of exposure: Findings from the National Health and Nutrition Examination Survey, 2001-2014. Environ Health 21, 23. [PubMed: 35139875]

[134]. Burns CJ, Beard KK, Cartmill JB (2001) Mortality in chemical workers potentially exposed to 2,4-dichlorophenoxyacetic acid (2,4-D) 1945–94: An update. Occup Environ Med 58, 24–30. [PubMed: 11119631]

[135]. de la Monte SM (2019) The full spectrum of Alzheimer's disease is rooted in metabolic derangements that drive type 3 diabetes. Adv Exp Med Biol 1128, 45–83. [PubMed: 31062325]

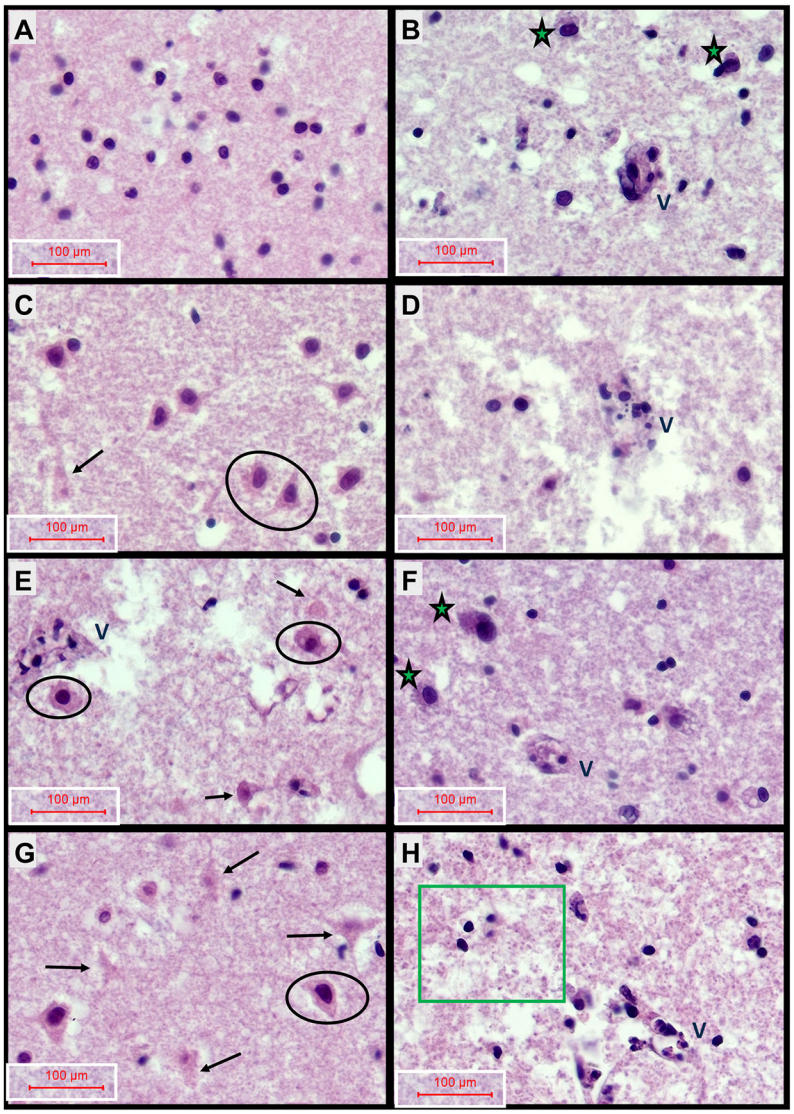

Fig. 1.

Neuropathological Effects of 2,4-D, 2,4,5-T, and *D* + T Treatment. Formalin-fixed paraffin-embedded, H&E-stained sections of rat frontal lobe slice cultures (FLSCs) treated with (A, B) Vehicle (DMSO-negative control), (C, D) 250 µg/ml of 2,4-D, (E, F) 250 µg/ml of 2,4,5-T, or (G, H) *D* + T (both agents) for 24 h. Cortex is shown in Panels A, C, E, G and white matter in Panels B, D, F, H. Vehicle-control (A) cortical tissue had abundant normal-appearing granule-type neurons with delicate cytoplasm, and (B) white matter with intact vessels (V) with prominent endothelial cells, moderately abundant oligodendrocytes (small round dark nuclei), and scattered larger reactive astrocytes (green asterisks). The 2,4-D treatments resulted in (C) cortical pathology characterized by neuronal injury/degeneration with cytoplasmic eosinophilia and nuclear hyperchromasia (examples circled), or apoptosis (arrow), and (D) white matter loss of oligodendrocytes (sparse cellularity relative to B), vascular necrosis (V-note endothelial nuclear fragmentation), and parenchymal degeneration (fragmentation-large irregular clear spaces). The 2,4,5-T treatments caused (E) cortical neuronal injury (circled) or apoptosis (arrows), and vascular necrosis (V), and (F) white

matter astrocyte activation (asterisks), but modest vascular and oligodendrocyte pathology. *D* + T treatment caused (G) abundant cortical neuronal degeneration with apoptosis (arrows) or injury (circled), and (H) conspicuous white matter degeneration (note abundant punctate swollen axons and tissue fragmentation), oligodendrocyte pyknosis (green box), and vascular necrosis (V-labeled). All images were photographed at 400×. The final image magnification scale bars are displayed.

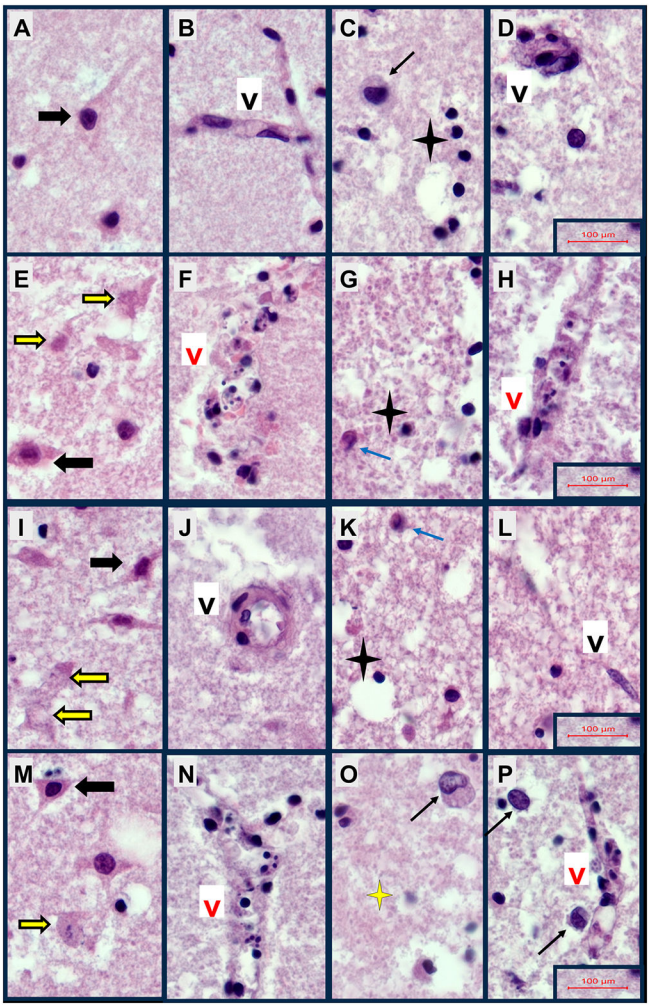

Fig. 2.

Cellular Neuropathology of FLSCs treated with 2,4-D, 2,4,5-T, or *D* + T. Formalin-fixed paraffin-embedded, H&E-stained histological sections of FLSCs treated with A–D) Vehicle, E–H) 250 μg/ml of 2,4-D, I-L) 250 μg/ml of 2,4,5-T, or M–P) *D* + T (both agents) for 24 h. Cortex (Panels A, B, E, F, I, J, M, N) showing relatively intact neurons (black arrows) or neurons with degenerative of apoptotic pathology (yellow arrows), and relatively intact vessels (Black 'V') or vascular necrosis (Red 'V'). White matter (Panels C, D, G, H, K, L, O, P) with normal round oligodendrocytes (black 4-point stars) or oligodendrocyte apoptosis (yellow 4-point star), reactive enlarged astrocyte (black arrows) or injured, eosinophilic astrocyte (blue arrow), intact vessels/vascular endothelial cells (Black 'V') or degenerated necrotic vessels (Red 'V'). Samples were photographed at 600x, then cropped and re-scaled. Final image magnification scale bars are displayed for each row.

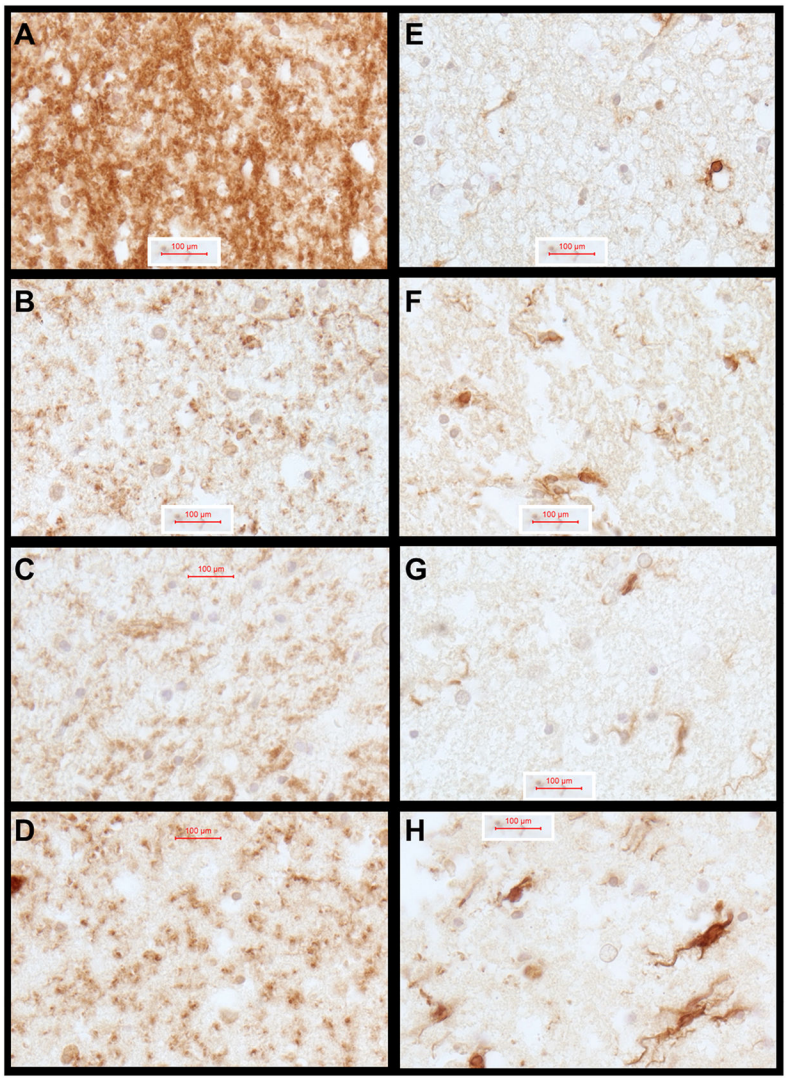

Fig. 3.

Agent Orange Herbicide Toxin Effects on Myelin-Oligodendrocyte Glycoprotein (MOG) and Glial Fibrillary Acidic Protein Expression in FLSCs: Adjacent formalin fixed, paraffin-embedded FLSC sections were immunostained for MOG1 (A–D) and GFAP (E–H) to evaluate the effects of (B, F) 2,4-D, (C, G) 2,4,5-T, and (D, H) *D* + T relative to (A, E) Vehicle control. Immunoreactivity was detected with the ImmPRESS Universal PLUS Polymer kit and DAB as the chromogen (brown precipitate). The sections were lightly counterstained with hematoxylin to show tissue architecture. Samples were photographed at 600x, then cropped and re-scaled. Final image magnification scale bars are displayed.

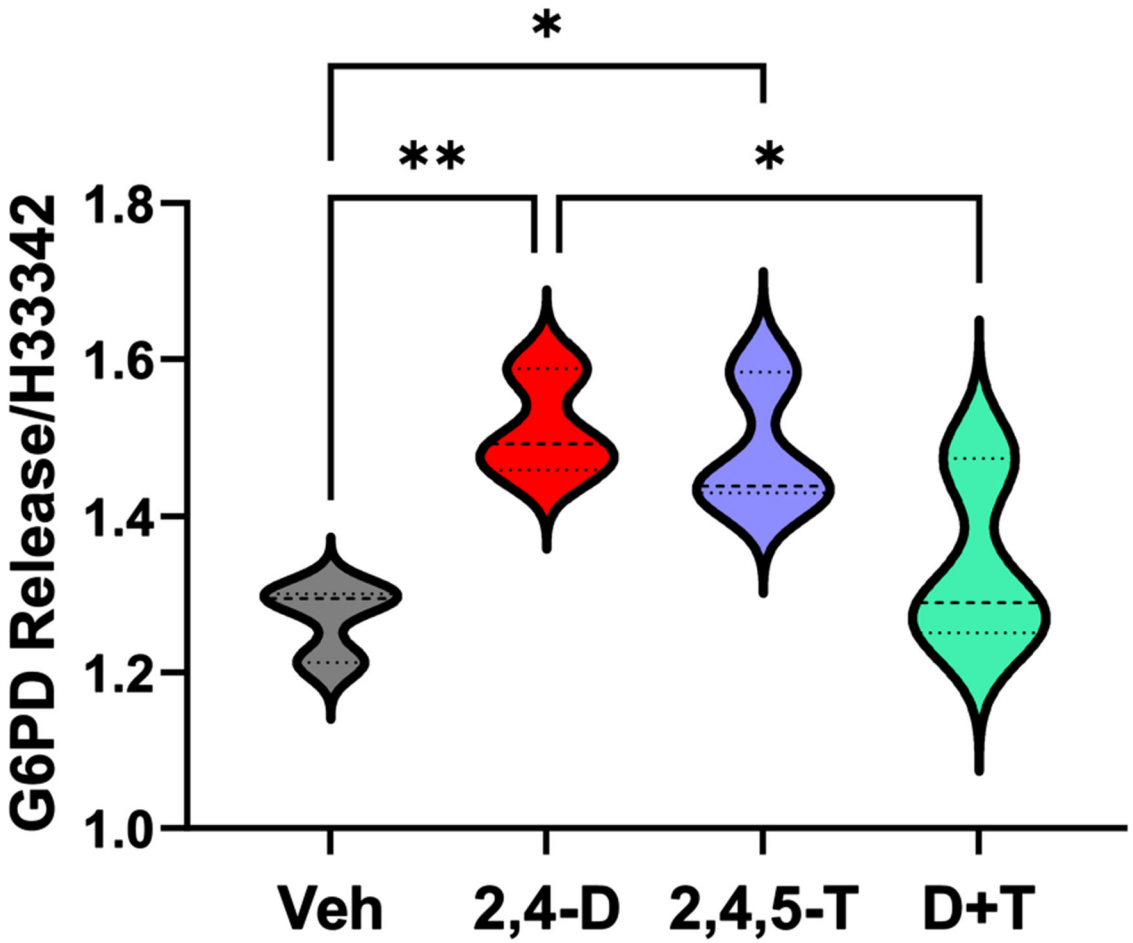

Fig. 4.

Cytotoxicity Assay Results. Culture supernatants from rat FLSCs treated for 24 h with Vehicle (Veh), 2,4-D, 2,4,5-T, or *D* + T were analyzed for G6PD release using the CyQuant Cytotoxicity Assay. Results were normalized to cellular content using H33342 fluorescence. Violin plots display data from 4 replicate cultures per group with each culture containing 4 or 5 frontal lobe slices (250 μm thick). Intergroup comparisons were made by one-way ANOVA (see Table 3) with post hoc multiple comparison Tukey tests. Significant differences are displayed (*$p < 0.05$; **$p < 0.01$).

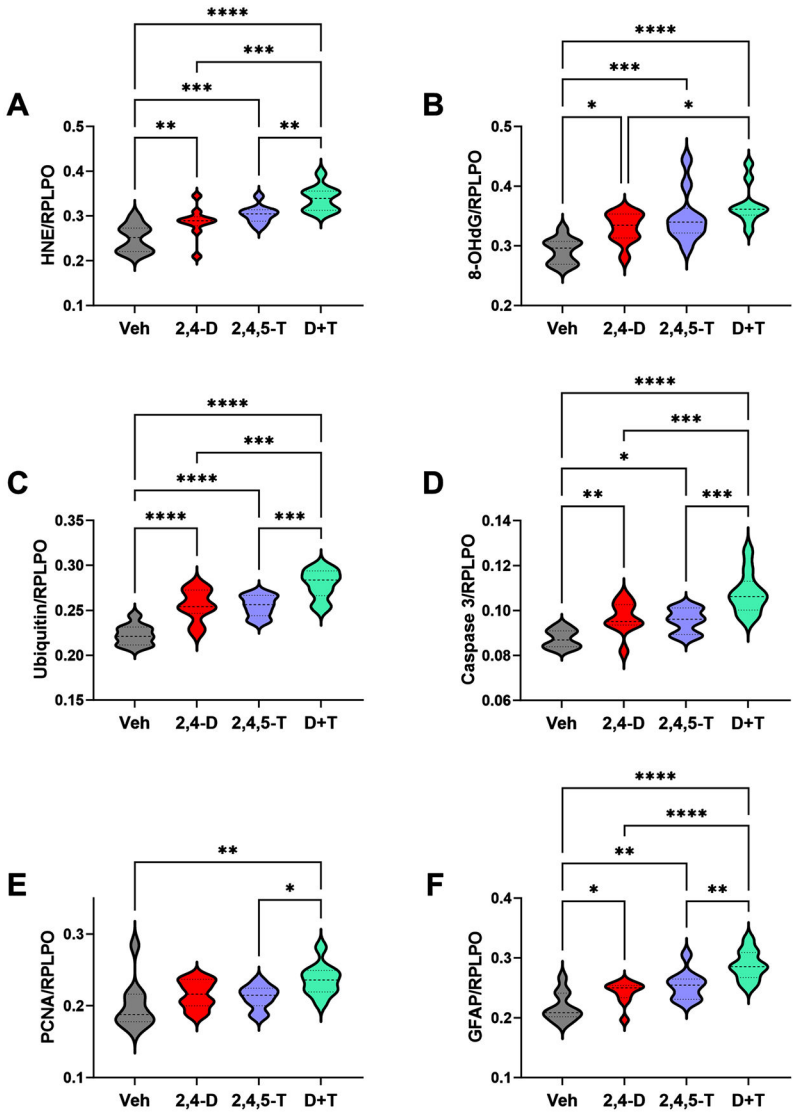

Fig. 5.

Metabolic and Oxidative Stress Indices Modulated by Agent Orange Herbicide Toxins. Rat FLSCs treated for 24 h with Vehicle (Veh), 2,4-D, 2,4,5-T, or *D* + T were analyzed for A) HNE, B) 8-OHdG, C) Ubiquitin, D) activated Caspase 3, E) PCNA, and F) GFAP immunoreactivity by duplex ELISA with results normalized to RPLPO. Each group included 6 replicate cultures with 5 or 6 frontal lobe slices per well. Results were analyzed by one-way ANOVA with post hoc Tukey tests (repeated measures; See Table 3). Significant *p*-values are indicated within the graphs (*$p < 0.05$; **$p < 0.01$; ***$p < 0.001$; ****$p < 0.0001$).

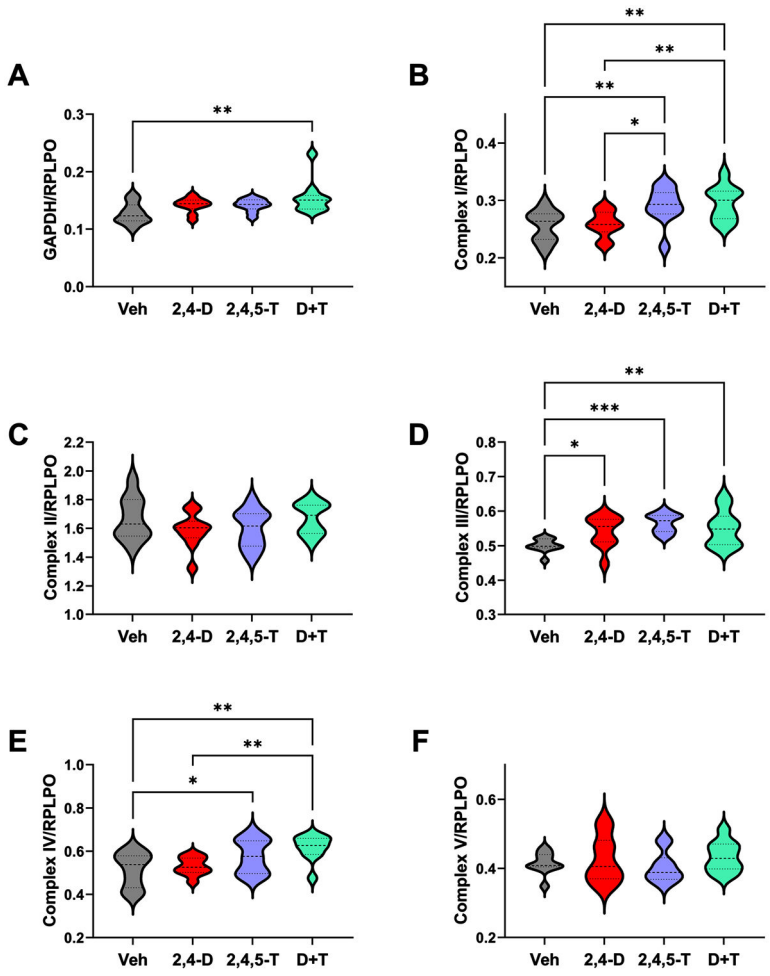

Fig. 6.

Effects of Agent Orange Herbicide Toxins on Mitochondrial Complex Protein Expression. Rat FLSCs treated for 24 h with Vehicle (Veh), 2,4-D, 2,4,5-T, or *D* + T were analyzed for A) GAPDH, B) Complex I, C) Complex II, D) Complex III, E) Complex IV, and F) Complex V immunoreactivity by duplex ELISA with results normalized to RPLPO. Each group included 6 replicate cultures with 5 or 6 frontal lobe slices per well. Results were analyzed by one-way ANOVA with post hoc Tukey tests (repeated measures; See Table 4). Significant *p*-values are indicated within the graphs (**p* < 0.05; ***p* < 0.01; ****p* < 0.001).

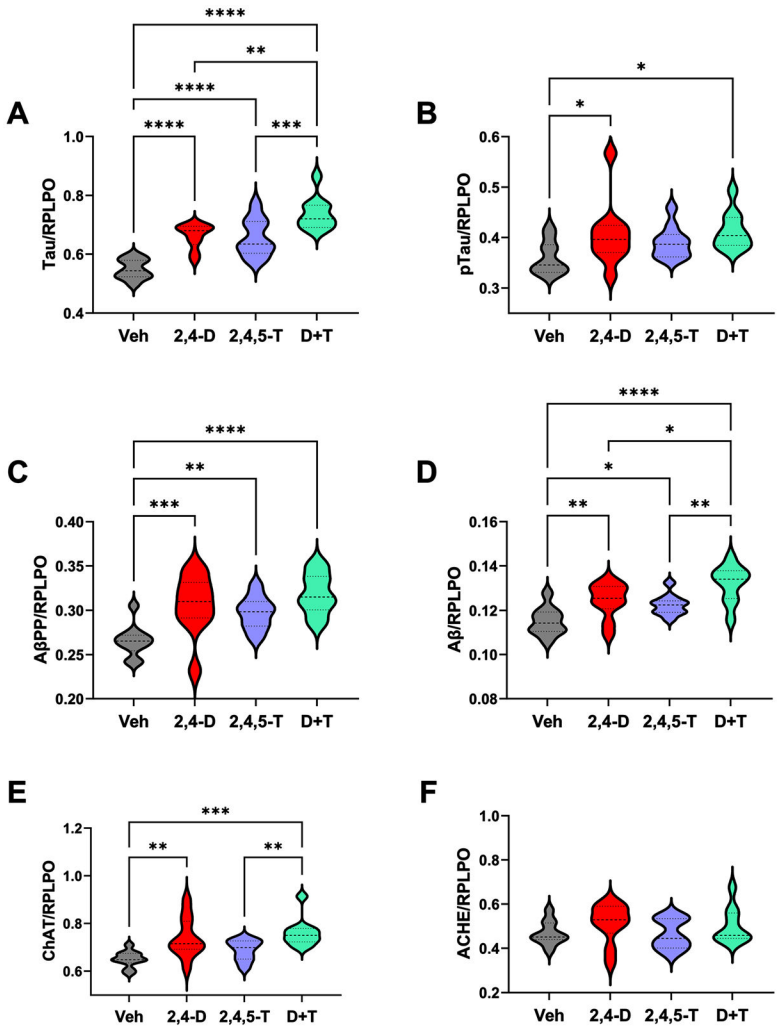

Fig. 7.

Effects of Agent Orange Herbicidal Toxin Exposures on AD Biomarker Expression. Rat FLSCs treated for 24 h with Vehicle (Veh), 2,4-D, 2,4,5-T, or *D* + T were analyzed for A) Tau, B) pTau-p^{S396}-Tau; PHF), C) AβPP, D) Aβ, E) ChAT, and F) AChE immunoreactivity by duplex ELISA with results normalized to RPLPO. Each group included 6 replicate cultures with 5 or 6 frontal lobe slices per well. Results were analyzed by one-way ANOVA with post hoc Tukey tests (repeated measures; See Table 5). Significant *p*-values are indicated within the graphs (*$p < 0.05$; **$p < 0.01$; ***$p < 0.001$; ****$p < 0.0001$).

Table 1

Agent Orange Herbicide Chemicals Used for Rat Frontal Lobe Slice Culture Experiments

Compound	Source	Catalog #	M.W.
2,4-Dichloro-phenoxy Acetic Acid (2,4-D)	Santa Cruz Biotechnologies, Dallas, TX, USA	sc-205097	221.04
2,4,5-Trichloro-phenoxyacetic acid (2,4,5-T)	Santa Cruz Biotechnologies, Dallas, TX, USA	sc-209335	255.48

Frontal lobe slice cultures were treated for 24 h with Vehicle, or the Agent Orange herbicidal toxins 2,4-D (250 μg/ml), 2,4,5-T (250 μg/ml), or both (each at 250 μg/ml). Vehicle treatments were with DMSO at the same final concentrations present in the Agent Orange-treated cultures. The 2,4-D and 2,4,5-T were purchased from Santa Cruz Biotechnologies, Dallas, TX, USA.

Table 2

Antibodies Used for Duplex ELISA Studies

Antibody	Type	Species	Stock	Final	Source	Catalog #
Tau	Polyclonal	Rabbit	6.2 mg/ml	1.55 μg/ml	Agilent/Dako, Santa Clara, CA	REF A0024
Phospho-Tau (pTau; p^{S396}-Tau) (PHF)	Monoclonal	Mouse	1.206 mg/ml	0.402 μg/ml	Cell Signaling, Danvers, MA	#9632S
Choline Acetyltransferase (ChAT)	Polyclonal	Rabbit	unknown	1 : 3000	Abcam, Waltham, MA	ab6168-100
Acetylcholinesterase (AChE)	Monoclonal	Mouse	1.0 mg/ml	0.25 μg/ml	Abcam, Waltham MA	ab2803
Amyloid Beta Precursor Protein-(AβPP)	Polyclonal	Rabbit	197 μg/ml	0.246 μg/ml	Cell Signaling, Danvers, MA	#2452
Amyloid-β Peptide of AβPP (Aβ)	Monoclonal	Mouse	200 μg/ml	0.4 μg/ml	Santa Cruz, Dallas, TX	sc-28365
8-Hydroxydeoxyguanosine (8-OHdG)	Monoclonal	Mouse	100 μg/ml	0.2 μg/ml	21st Century Biochemicals, Marlborough, MA	unknown
4-Hydroxy-2-nonenal (HNE)	Polyclonal	Goat	0.8 mg/ml	1.6 μg/ml	Abcam, Waltham, MA	ab46544
Glial Fibrillary Acidic Protein (GFAP)	Monoclonal	Mouse	1 mg/ml	4 μg/ml	Molecular Probes (Invitrogen)	A21282
Glyceraldehyde-3-phosphate dehydrogenase (GAPDH)	Monoclonal	Mouse	200 μg/ml	0.2 μg/ml	Santa Cruz, Dallas, TX	sc-365062
Ubiquitin (UBQ)	Polyclonal	Rabbit	0.25 mg/ml	0.5 μg/ml	Abcam, Waltham, MA	ab7780-500
Mitochondrial Complex I	Monoclonal	Mouse	0.5 mg/ml	2 μg/ml	Molecular Probes-Invitrogen, Eugene, OR	A21344
Mitochondrial Complex II	Monoclonal	Mouse	0.5 mg/ml	0.125 μg/ml	Molecular Probes-Invitrogen, Eugene, OR	A11142
Mitochondrial Complex III	Monoclonal	Mouse	0.5 mg/ml	0.5 μg/ml	Molecular Probes-Invitrogen, Eugene, OR	A11143
Mitochondrial Complex IV	Monoclonal	Mouse	0.5 mg/ml	0.125 μg/ml	Molecular Probes-Invitrogen, Eugene, OR	A21348
Mitochondrial Complex V	Monoclonal	Mouse	1.0 mg/ml	0.33 μg/ml	Molecular Probes-Invitrogen, Eugene, OR	A21351
Myelin Associated Glycoprotein 1 (MOG1)	Polyclonal	Rabbit	1.0 mg/ml	2.0 μg/ml	Abcam, Waltham, MA	ab32760
RPLPO	Monoclonal	Mouse	100 μg/ml	0.1 μg/ml	Santa Cruz, Dallas, TX	sc-293260

Table 3

Biomarkers of Oxidative Stress and Injury/Damage

Biomarker	F-Ratio	*p*	Linear Trend (r^2)	*p*
G6PD Release	5.70	**0.022**	0.026	N.S.
HNE	16.56	**<0.0001**	0.9834	**<0.0001**
8-OHdG	10.38	**<0.0001**	0.9645	**<0.0001**
Ubiquitin	26.27	**<0.0001**	0.8780	**<0.0001**
Caspase 3	15.60	**<0.0001**	0.8539	**<0.0001**
PCNA	4.013	**0.0146**	0.8043	**0.0036**
GFAP	15.97	**<0.0001**	0.9675	**<0.0001**

G6PD release was measured in culture supernatant fluid after 24 h treatment with results normalized. Duplex ELISAs measured immunoreactivity in rat FLSC homogenates (n = 6/group) treated with vehicle, 2,4-D, 2,4,5-T, or 2,4-D plus 2,4,5-T (D + T) for 24 h. Immunoreactivity normalized to RPLPO was used for inter-group comparisons by one-way ANOVA (DFn, DFd = 3, 36). Linear trend analysis (r^2) for the slope reflecting progressive quantitative shifts in protein expression from Vehicle to 2,4-D, to 2,4,5-T, to D + T treatment. p-values<0.05 were considered statistically significant. N.S., not significant. See Fig. 2 for graphed results with post-hoc Tukey multiple comparisons results. PCNA, proliferating cell nuclear antigen; 8-OHdG, 8-hydroxyguanosine; 4-HNE, 4-hydroxy-2-nonenal; GFAP, glial fibrillary acidic protein.

J Alzheimers Dis. Author manuscript; available in PMC 2024 July 01.

Table 4

Mitochondrial Function

Biomarker	F-Ratio	*p*	Linear Trend (r^2)	p
GAPDH	3.631	**0.0218**	0.8996	**0.0035**
Complex I	5.599	**0.0029**	0.8660	**0.0005**
Complex II	1.191	N.S.	0.0044	N.S.
Complex III	5.267	**0.0041**	0.6425	**0.003**
Complex IV	4.758	**0.0068**	0.9644	**0.0007**
Complex V	0.714	N.S.	0.1003	N.S.

Duplex ELISAs measured immunoreactivity in rat FLSC homogenates (n = 6/group) treated with vehicle, 2,4-D, 2,4,5-T, or 2,4-D plus 2,4,5-T (D + T) for 24 h. Immunoreactivity normalized to RPLPO was used for inter-group comparisons by one-way ANOVA (DFn, DFd = 3, 36). Linear trend analysis (r^2) was calculated for the slope reflecting quantitative shifts in protein expression from Vehicle to 2,4-D, to 2,4,5-T, to D + T treatment. p-values<0.05 were considered statistically significant (bold font). See Fig. 4 for graphed results with post-hoc Tukey multiple comparisons results. GAPDH, glyceraldehyde-3-phosphate dehydrogenase; Complex, Mitochondrial Complexes I-V.

Table 5

Biomarkers of Neurodegeneration

Biomarker	F-Ratio	*p*	Linear Trend (r^2)	P
Tau	24.55	**<0.0001**	0.8679	**<0.0001**
pTau	2.879	**0.0493**	0.6206	**0.0264**
pTau/Tau	3.659	**0.0212**	0.9661	**0.0025**
AβPP	8.887	**0.0002**	0.7190	**<0.0001**
Aβ	10.59	**<0.0001**	0.8149	**<0.0001**
ChAT	7.186	**0.0007**	0.5255	**0.0018**
AChE	1.123	N.S.	0.056	N.S.

Duplex ELISAs measured immunoreactivity in rat FLSCs (n = 6/group) treated with vehicle, 2,4-D, 2,4,5-T, or 2,4-D plus 2,4,5-T (D + T) for 24 h. Immunoreactivity normalized to RPLPO was used for inter-group comparisons by one-way ANOVA (DFn, DFd = 3, 36). Linear trend analysis (r^2) was calculated for the slope reflecting quantitative shifts in protein expression from Vehicle to 2,4-D, to 2,4,5-T, to D + T. p-values<0.05 were considered statistically significant (bold font). See Fig. 4 for graphed results with post-hoc Tukey multiple comparisons results. AβPP, amyloid-beta protein precursor; Aβ, amyloid-beta C-terminal fragment of AβPP; pTau, (S396) phosphorylated tau; ChAT, choline acetyltransferase; AChE, acetylcholinesterase.